An Interior-Point Method for Large-Scale ℓ_1-Regularized Logistic Regression

Kwangmoo Koh   Seung-Jean Kim   Stephen Boyd

Information Systems Laboratory

Electrical Engineering Department, Stanford University

Stanford, CA 94305-9510

deneb1@stanford.edu   sjkim@stanford.edu   boyd@stanford.edu

July 9, 2006

Abstract

Logistic regression with ℓ_1 regularization has been proposed as a promising method for feature selection in classification problems. In this paper we describe an efficient interior-point method for solving large-scale ℓ_1-regularized logistic regression problems. Small problems with up to a thousand or so features and examples can be solved in seconds on a PC; medium sized problems, with tens of thousands of features and examples, can be solved in tens of seconds (assuming some sparsity in the data). A variation on the basic method, that uses a preconditioned conjugate gradient method to compute the search step, can solve very large problems, with a million features and examples (*e.g.*, the 20 Newsgroups data set), in a few tens of minutes, on a PC. Using warm-start techniques, a good approximation of the entire regularization path can be computed much more efficiently than by solving a family of problems independently.

Key words: logistic regression, feature selection, ℓ_1 regularization, regularization path, interior-point methods.

Contents

1 Introduction

1.1 Logistic regression

Let $x \in \mathbf{R}^n$ denote a vector of explanatory or feature variables, and $b \in \{-1, +1\}$ denote the associated binary output or outcome. The logistic model has the form

$$\mathrm{Prob}(b|x) = \frac{1}{1 + \exp\left(-b(w^T x + v)\right)} = \frac{\exp\left(b(w^T x + v)\right)}{1 + \exp\left(b(w^T x + v)\right)},$$

where $\mathrm{Prob}(b|x)$ is the conditional probability of b, given $x \in \mathbf{R}^n$. The logistic model has parameters $v \in \mathbf{R}$ (the intercept) and $w \in \mathbf{R}^n$ (the weight vector). When $w \neq 0$, $w^T x + v = 0$ defines the neutral hyperplane in feature space, on which the conditional probability of each outcome is 1/2. On the shifted parallel hyperplane $w^T x + v = 1$, which is a distance $1/\|w\|_2$ from the neutral hyperplane, the conditional probability of outcome $b = 1$ is $1/(1 + 1/e) \approx 0.73$, and the conditional probability of $b = -1$ is $1/(1 + e) \approx 0.27$. On the hyperplane $w^T x + v = -1$, these conditional probabilities are reversed. As $w^T x + v$ increases above one, the conditional probability of outcome $b = 1$ rapidly grows large; as $w^T x + v$ decreases below -1, the conditional probability of outcome $b = 1$ rapidly becomes large. The slab in feature space defined by $|w^T x + v| \leq 1$ defines the *ambiguity region*, in which there is substantial probability of each outcome; outside this slab, one outcome is much more likely than the other.

Suppose we are given a set of (observed or training) examples,

$$(x_i, b_i) \in \mathbf{R}^n \times \{-1, +1\}, \quad i = 1, \ldots, m,$$

assumed to be independent samples from a distribution. We use $p_{\mathrm{log}}(v, w) \in \mathbf{R}^m$ to denote the vector of conditional probabilities, according to the logistic model,

$$p_{\mathrm{log}}(v, w)_i = \mathrm{Prob}(b_i|x_i) = \frac{\exp(w^T a_i + v b_i)}{1 + \exp(w^T a_i + v b_i)}, \quad i = 1, \ldots, m, \tag{1}$$

where $a_i = b_i x_i$. The likelihood function associated with the samples is $\prod_{i=1}^m p_{\mathrm{log}}(v, w)_i$, and the log-likelihood function is given by

$$\sum_{i=1}^m \log p_{\mathrm{log}}(v, w)_i = -\sum_{i=1}^m f(w^T a_i + v b_i),$$

where f is the *logistic loss function*

$$f(z) = \log(1 + \exp(-z)). \tag{2}$$

This loss function is convex, so the log-likelihood function is concave. The negative of the log-likelihood function is called the *(empirical) logistic loss*, and dividing by m we obtain the *average logistic loss*,

$$l_{\mathrm{avg}}(v, w) = (1/m) \sum_{i=1}^m f(w^T a_i + v b_i).$$

We can determine the model parameters w and v by maximum likelihood estimation from the observed examples, by solving the convex optimization problem

$$\text{minimize} \quad l_{\text{avg}}(v, w), \tag{3}$$

with variables $v \in \mathbf{R}$ and $w \in \mathbf{R}^n$, and problem data $A = [a_1 \ \cdots \ a_m]^T \in \mathbf{R}^{m \times n}$ and the vector of binary outcomes $b = [b_1 \ \cdots \ b_m]^T \in \mathbf{R}^m$. The problem (3) is called the *logistic regression problem* (LRP).

The average logistic loss is always nonnegative, *i.e.*, $l_{\text{avg}}(v, w) \geq 0$, since $f(z) \geq 0$ for any z. For the choice $w = 0$, $v = 0$, we have $l_{\text{avg}}(0, 0) = \log 2 \approx 0.693$, so the optimal value of the LRP lies between 0 and $\log 2$. In particular, the optimal value can range (roughly) between 0 and 1. The optimal value is 0 only when the original data are linearly separable, *i.e.*, there exist w and v such that $w^T x_i + v > 0$ when $b_i = 1$, and $w^T x_i + v < 0$ when $b_i = -1$. In this case the optimal value of the LRP (3) is not achieved (except in the limit with w and v growing arbitrarily large). The optimal value is $\log 2$, *i.e.*, $w = 0$, $v = 0$ are optimal, only if $\sum_{i=1}^m b_i = 0$ and $\sum_{i=1}^m a_i = 0$. (This follows from the expression for ∇l_{avg}, given in §2.1.) This occurs only when the number of positive examples (*i.e.*, those for which $b_i = 1$) is equal to the number of negative examples, and the average of x_i over the positive examples is the negative of the average value of x_i over the negative examples.

The LRP (3) is a smooth convex optimization problem, and can be solved by a wide variety of methods, such as gradient descent, steepest descent, Newton, quasi-Newton, or conjugate-gradients (CG) methods.

Once we find maximum likelihood values of v and w, *i.e.*, a solution of (3), we can predict the probability of the two possible outcomes, given a new feature vector $x \in \mathbf{R}^n$, using the associated logistic model. For example, when $w \neq 0$, we can form the logistic classifier

$$\phi(x) = \text{sgn}(w^T x + v), \tag{4}$$

where

$$\text{sgn}(z) = \begin{cases} +1 & z > 0 \\ -1 & z \leq 0, \end{cases}$$

which picks the more likely outcome, given x, according to the logistic model. This classifier is linear, meaning that the boundary between the two decision outcomes is a hyperplane (defined by $w^T x + v = 0$).

1.2 ℓ_2-regularized logistic regression

When m, the number of observations or training examples, is not large enough compared to n, the number of feature variables, simple logistic regression leads to over-fit. That is, the classifier found by solving the LRP (3) performs perfectly (or very well) on the training examples, but may perform poorly on unseen examples. Over-fitting tends to occur when the fitted model has many feature variables with (relatively) large weights in magnitude, *i.e.*, w is large.

A standard technique to prevent over-fitting is *regularization*, in which an extra term that penalizes large weights is added to the average logistic loss function. The ℓ_2*-regularized logistic regression problem* is

$$\text{minimize} \quad l_{\text{avg}}(v,w) + \lambda \|w\|_2^2 = (1/m)\sum_{i=1}^m f(w^T a_i + v b_i) + \lambda \sum_{i=1}^n w_i^2. \qquad (5)$$

Here $\lambda > 0$ is the regularization parameter, used to control the trade-off between the average logistic loss and the size of the weight vector, as measured by the ℓ_2-norm. No penalty term is imposed on the intercept, since it is a parameter for thresholding the weighted sum $w^T x$ in the linear classifier (4). The solution of the ℓ_2-regularized regression problem (5) (which exists and is unique) can be interpreted in a Bayesian framework, as the maximum a posteriori probability (MAP) estimate of w and v, when w has a Gaussian prior distribution; see, *e.g.*, [10, 28].

The objective function in the ℓ_2-regularized LRP is smooth and convex, and so (like the ordinary, unregularized LRP) can be minimized by standard methods such as gradient descent, steepest descent, Newton, quasi-Newton, truncated Newton, or CG methods (see, *e.g.*, [41, 37]). Other methods that have been used include optimization transfer [32, 60], and the iteratively re-weighted least squares (IRWLS) method [30]. Newton's method and variants are very effective for small and medium sized problems, while conjugate-gradients and limited memory Newton (or truncated Newton) methods can handle very large problems. Truncated Newton methods have been applied to large-scale problems in several other fields, *e.g.*, image restoration [21] and support vector machines [29]. For large-scale iterative methods such as truncated Newton or CG, the convergence typically improves as the regularization parameter λ is increased, since (roughly speaking) this makes the objective more quadratic, and improves the conditioning of the problem.

1.3 ℓ_1-regularized logistic regression

More recently, ℓ_1*-regularized logistic regression* has received much attention. The ℓ_1-regularized logistic regression problem is

$$\text{minimize} \quad l_{\text{avg}}(v,w) + \lambda \|w\|_1 = (1/m)\sum_{i=1}^m f(w^T a_i + v b_i) + \lambda \sum_{i=1}^n |w_i|, \qquad (6)$$

where $\lambda > 0$ is the regularization parameter. The only difference with ℓ_2-regularized logistic regression is that we measure the size of w by its ℓ_1-norm, instead of its ℓ_2-norm. A solution of the ℓ_1-regularized logistic regression must exist, but it need not be unique. Any solution of the ℓ_1-regularized logistic regression problem (6) can be interpreted in a Bayesian framework as a MAP estimate of w and v, when w has a Laplacian prior distribution; see, *e.g.*, [10, 28]. The objective function in the ℓ_1-regularized LRP (6) is convex, but not differentiable (specifically, when any of the weights is zero), so solving it is more of a computational challenge than solving the ℓ_2-regularized LRP (5).

Despite the additional computational challenge posed by ℓ_1-regularized logistic regression, compared to ℓ_2-regularized logistic regression, interest in its use has been growing. The main motivation is that ℓ_1-regularized LR typically yields a *sparse* vector w, *i.e.*, w typically has relatively few nonzero coefficients. (In contrast, ℓ_2-regularized LR typically yields w with all coefficients nonzero.) When $w_j = 0$, the associated logistic model does not use the jth component of the feature vector, so sparse w corresponds to a logistic model that uses only a few of the features, *i.e.*, components of the feature vector. Indeed, we can think of a sparse w as a *selection* of the relevant or important features (*i.e.*, those associated with nonzero w_j), as well as the choice of the intercept value and weights (for the selected features). A logistic model with sparse w is, in a sense, simpler or more parsimonious than one with nonsparse w. It is not surprising that ℓ_1-regularized LR can outperform ℓ_2-regularized LR, especially when the number of observations is smaller than the number of features [40].

We refer to the number of nonzero components in w as its *cardinality*, denoted $\mathrm{card}(w)$. Thus, ℓ_1-regularized LR tends to yield w with $\mathrm{card}(w)$ small; the regularization parameter λ roughly controls $\mathrm{card}(w)$, with larger λ typically (but not always) yielding smaller $\mathrm{card}(w)$.

The general idea of ℓ_1 regularization for the purposes of model or feature selection (or just sparsity of solution) is quite old, and widely used in other contexts. In statistics, it is used in the well-known Lasso algorithm [51] for ℓ_1-regularized linear regression, and its extensions such as the fused Lasso [52, 53]. The idea also comes up in signal processing (basis pursuit [11, 12] and wavelet thresholding [19]), portfolio optimization [34], control design [26], computer-aided design of integrated circuits [9, 56], and machine learning (sparse principal component analysis [15], maximum likelihood estimation of graphical models [5, 14], boosting [47], and ℓ_1-SVM [61]). A recent survey of the idea can be found in [54]. In [18, 54], the authors give some theoretical analysis of why ℓ_1 regularization leads to a sparse model in linear regression.

To solve the ℓ_1-regularized LRP (6), generic methods for nondifferentiable convex problems can be used, such as the ellipsoid method or subgradient methods [50, 44]. These methods are usually very slow in practice, however. (Because ℓ_1-regularized LR typically results in a weight vector with (many) zero components, we cannot simply ignore the nondifferentiability of the objective in the ℓ_1-regularized LRP (6), hoping to not encounter points of nondifferentiability.)

Faster methods are based on transforming the problem to an equivalent one, with linear inequality constraints,

$$\begin{array}{ll} \text{minimize} & l_{\mathrm{avg}}(v,w) + \lambda \mathbf{1}^T u, \\ \text{subject to} & -u_i \le w_i \le u_i, \quad i = 1, \ldots, n, \end{array} \tag{7}$$

where the variables are the original ones $v \in \mathbf{R}$, $w \in \mathbf{R}^n$, along with $u \in \mathbf{R}^n$. Here $\mathbf{1}$ denotes the vector with all components one, so $\mathbf{1}^T u$ is the sum of the components of u. (To see the equivalence with the ℓ_1-regularized LRP (6), we note that at the optimal point for (7), we must have $u_i = |w_i|$, in which case the objectives in (7) and (6) are the same.) The reformulated problem (7) is a convex optimization problem, with a smooth objective, and linear constraint functions, so it can be solved by standard convex optimization methods such as SQP, augmented Lagrangian, interior-point, and other methods. High quality solvers that can directly handle the problem (7) (and therefore, carry out ℓ_1-regularized LR) include for example LOQO [57], LANCELOT [13], MOSEK [36], and NPSOL [24]. These general purpose solvers can solve small and medium scale ℓ_1-regularized LRPs quite effectively. Other recent work on computational methods for ℓ_1-regularized logistic regression includes bound optimization algorithms [31], online algorithms [4], coordinate descent methods [22], and the Gauss-Seidel method [49].

The main goal of this paper is to describe a specialized method for solving the ℓ_1-regularized logistic regression problem that is very efficient, for all size problems. In particular our method handles very large problems, and is not much slower than the fastest large-scale methods (conjugate-gradients and limited memory Newton) applied to the ℓ_2-regularized LRP. In this paper we focus on methods for *solving* the ℓ_1-regularized LRP; we do not discuss the benefits or advantages of ℓ_1-regularized LR, compared to ℓ_2-regularized LR or other methods for modeling or constructing classifiers for two-class data.

1.4 Regularization path

Let $(v^\star_\lambda, w^\star_\lambda)$ be a solution for the ℓ_1-regularized LRP with regularization parameter λ. The family of solutions, as λ varies over $(0, \infty)$, is called the (ℓ_1-) *regularization path*. In many practical applications, the regularization path (or some portion) needs to be computed, in order to determine an appropriate value of λ. At the very least, the ℓ_1-regularized LRP must solved for multiple, and often many, values of λ.

In ℓ_1-regularized linear regression, which is the problem of minimizing

$$\|Fz - g\|_2^2 + \lambda \|z\|_1$$

over the variable z, where $\lambda > 0$ is the regularization parameter, it can be shown that the regularization path is piecewise linear, with kinks at each point where any component of the variable z transitions from zero to nonzero, or vice versa. Using this fact, the entire regularization path in a (small or medium size) ℓ_1-regularized linear regression problem can be computed efficiently; see, *e.g.*, [27, 20, 46, 42].

In [43], the authors describe an algorithm for (approximately) computing the entire regularization path for general linear models (GLMs) including logistic regression models. In [46], a general path following method based on a predictor-corrector method is described for general regularized convex loss minimization problems. These methods are related to numerical continuation techniques for following piecewise smooth curves, which have been well studied in the optimization literature [1]. All path-following methods are slow for large-scale problems, where the number of kinks or events is very large (at least n). When the number of kinks on the portion of the regularization path of interest is modest, however, these path-following methods can be very fast, requiring just a small multiple of the effort needed to solve one regularized problem to compute the whole path (or a portion).

In this paper we will describe a fast method for computing a large number of points on the regularization path, using a warm-start technique and our interior-point method. Unlike the methods mentioned above, our method does not attempt to track the path exactly (*i.e.*, jumping from kink to kink on the path); it remains efficient even when successive values of λ jump over many kinks. This is essential when computing the regularization path in a large-scale problem. Our method allows us to compute a large number of points (but much fewer than n, when n is very large) on the regularization path, much more efficiently than by solving a family the problems independently.

1.5 Standardization

Standardization is a widely used pre-processing step applied to the feature vector, so that each (transformed) feature has zero mean and unit variance (over the examples). The mean feature vector is $\mu = (1/m)\sum_{i=1}^m x_i$, and the vector of feature standard deviations σ is defined by

$$\sigma_j = \left((1/m) \sum_{i=1}^m (x_{ij} - \mu_j)^2 \right)^{1/2}, \quad j = 1, \ldots, n,$$

where x_{ij} is the jth component of x_i. The *standardized feature vector* is defined as

$$x^{\mathrm{std}} = \mathbf{diag}(\sigma)^{-1}(x - \mu).$$

When the examples are standardized, we obtain the standardized data matrix

$$A^{\mathrm{std}} = \mathbf{diag}(b)(X - \mathbf{1}\mu^T)\,\mathbf{diag}(\sigma)^{-1} = A\,\mathbf{diag}(\sigma)^{-1} - b\mu^T\,\mathbf{diag}(\sigma)^{-1}, \tag{8}$$

where $X = [x_1 \cdots x_m]^T$. We carry out logistic regression (possibly regularized) using the data matrix A^{std} in place of A, to obtain (standardized) logistic model parameters w^{std}, v^{std}. In terms of the original feature vector, our logistic model is

$$\mathrm{Prob}(b|x) = \frac{1}{1 + \exp\left(-b(w^{\mathrm{std}\,T} x^{\mathrm{std}} + v^{\mathrm{std}})\right)} = \frac{1}{1 + \exp\left(-b(w^T x + v)\right)}$$

where

$$w = \mathbf{diag}(\sigma)^{-1} w^{\mathrm{std}}, \qquad v = v^{\mathrm{std}} - w^{\mathrm{std}\,T}\,\mathbf{diag}(\sigma)^{-1}\mu.$$

We point out one subtlety here related to sparsity of the data matrix. For small or medium sized problems, or when the original data matrix A is dense, forming the standardized data matrix A^{std} does no harm. But when the original data matrix A is sparse, which is the key to efficient solution of large-scale ℓ_1-regularized LRPs, forming A^{std} is disastrous, since A^{std} is in general dense, even when A is sparse.

But we will get around this problem, when working with very large problems, by never actually forming the matrix A^{std}. (This is explained in §5.)

1.6 Outline

In §2, we give (necessary and sufficient) optimality conditions, and a dual problem, for the ℓ_1-regularized LRP. Using the dual problem, we show how to compute a lower bound on the suboptimality of any pair (v, w). We describe our basic interior-point method in §3, and demonstrate its performance in §4 with small and medium scale synthetic and machine learning benchmark examples. We show that ℓ_1-regularized LR can be carried out within around 35 or so iterations, where each iteration has the same complexity as solving an ℓ_2-regularized linear regression problem.

In §5, we describe a variation on our basic method that uses a preconditioned conjugate gradient approach to compute the search direction. This variation on our method can solve very large problems, with a million features and examples (*e.g.*, the 20 Newsgroups data set), in under an hour, on a PC, provided the data matrix is sufficiently sparse.

In §6, we consider the problem computing the regularization path efficiently, at a variety of values of λ (but potentially far fewer than the number of kinks on the path). Using warm-start techniques, we show how this can done much more efficiently than by solving a family of problems independently. we show how this can be done much more efficiently than by solving a family of problems independently. In §7, we describe generalizations of our method to other ℓ_1-regularized convex loss minimization problems.

2 Optimality conditions and dual

2.1 Optimality conditions

The objective function of the ℓ_1-regularized LRP, $l_{\text{avg}}(v, w) + \lambda\|w\|_1$, is convex but not differentiable, so we use a first-order optimality condition based on subdifferential calculus (see, *e.g.*, [6, Prop. B.24] or [7, §2]). The average logistic loss is differentiable, with

$$\begin{aligned}\nabla_v l_{\text{avg}}(v, w) &= (1/m)\sum_{i=1}^m f'(w^T a_i + v b_i) b_i \\ &= -(1/m)\sum_{i=1}^m (1 - p_{\log}(v, w)_i) b_i \\ &= -(1/m) b^T(\mathbf{1} - p_{\log}(v, w)),\end{aligned}$$

and

$$\begin{aligned}\nabla_w l_{\text{avg}}(v, w) &= (1/m)\sum_{i=1}^m f'(w^T a_i + v b_i) a_i \\ &= -(1/m)\sum_{i=1}^m (1 - p_{\log}(v, w)_i) a_i \\ &= -(1/m) A^T(\mathbf{1} - p_{\log}(v, w)).\end{aligned}$$

The subdifferential of $\|w\|_1$ is given by

$$(\partial\|w\|_1)_i = \begin{cases} \{1\} & w_i > 0, \\ \{-1\} & w_i < 0, \\ [-1, 1] & w_i = 0. \end{cases}$$

The necessary and sufficient condition for (v, w) to be optimal for the ℓ_1-regularized LRP (6) is

$$\nabla_v l_{\text{avg}}(v, w) = 0, \qquad 0 \in \nabla_w l_{\text{avg}}(v, w) + \lambda \partial \|w\|_1,$$

which can be expressed as

$$b^T(\mathbf{1} - p_{\text{log}}(v, w)) = 0, \tag{9}$$

and

$$(1/m)\left(A^T(\mathbf{1} - p_{\text{log}}(v, w))\right)_i \in \begin{cases} \{+\lambda\} & w_i > 0, \\ \{-\lambda\} & w_i < 0, \\ [-\lambda,\, \lambda] & w_i = 0, \end{cases} \quad i = 1, \ldots, n. \tag{10}$$

Let us analyze when a pair of the form $(v, 0)$ is optimal. This occurs if and only if

$$b^T(\mathbf{1} - p_{\text{log}}(v, 0)) = 0, \qquad \|(1/m)A^T(\mathbf{1} - p_{\text{log}}(v, 0))\|_\infty \leq \lambda.$$

The first condition is equivalent to $v = \log(m_+/m_-)$, where m_+ is the number of training examples with outcome 1 (called positive) and m_- is the number of training examples with outcome -1 (called negative). Using this value of v, the second condition becomes

$$\lambda \geq \lambda_{\max} = \|(1/m)A^T(\mathbf{1} - p_{\text{log}}(\log(m_+/m_-), 0))\|_\infty. \tag{11}$$

The number $\lambda_{\max}$ gives us an upper bound on the useful range of the regularization parameter λ: For any larger value of λ, the logistic model obtained from ℓ_1-regularized LR has weight zero, which has no ability to classify. Put another way, for $\lambda \geq \lambda_{\max}$, we get a maximally sparse weight vector, *i.e.*, one with $\text{card}(w) = 0$.

We can give a more explicit formula for $\lambda_{\max}$:

$$\lambda_{\max} = (1/m)\left\| \frac{m_-}{m} \sum_{b_i=1} a_i + \frac{m_+}{m} \sum_{b_i=-1} a_i \right\|_\infty = (1/m)\left\| X^T \tilde{b} \right\|_\infty,$$

where

$$\tilde{b}_i = \begin{cases} m_-/m & b_i = 1 \\ -m_+/m & b_i = -1, \end{cases} \quad i = 1, \ldots, m.$$

Thus, $\lambda_{\max}$ is a maximum correlation between the individual features and the (weighted) output vector $\tilde{b}$. When the features have been standardized, we have $\sum_{i=1}^m x_i = 0$, so we get the simplified expression

$$\lambda_{\max} = (1/m)\left\| \sum_{b_i=1} x_i \right\|_\infty = (1/m)\left\| \sum_{b_i=-1} x_i \right\|_\infty.$$

2.2 Dual problem

To derive a Lagrange dual of the ℓ_1-regularized LRP (6), we first introduce a new variable $z \in \mathbf{R}^m$, as well as new equality constraints $z_i = w^T a_i + vb_i$, $i = 1, \ldots, m$, to obtain the equivalent problem

$$\begin{array}{ll} \text{minimize} & (1/m)\sum_{i=1}^m f(z_i) + \lambda\|w\|_1 \\ \text{subject to} & z_i = w^T a_i + vb_i, \quad i = 1, \ldots, m. \end{array} \tag{12}$$

Associating dual variables $\nu_i \in \mathbf{R}$ with the equality constraints, the Lagrangian is

$$L(v, w, z, \nu) \;=\; (1/m)\sum_{i=1}^m f(z_i) + \lambda\|w\|_1 + \nu^T(-z + Aw + bv).$$

The dual function is

$$\begin{aligned} \inf_{v,w,z} L(v, w, z, \nu) &= (1/m)\inf_z \sum_{i=1}^m (f(z_i) - m\nu_i z_i) + \inf_w \left(\lambda\|w\|_1 + \nu^T A w\right) + \inf_v \nu^T b v \\ &= \begin{cases} -(1/m)\sum_{i=1}^m f^*(-m\nu_i) & \|A^T\nu\|_\infty \le \lambda, \quad b^T\nu = 0, \\ -\infty & \text{otherwise,} \end{cases} \end{aligned}$$

where f^* is the *conjugate* of the logistic loss function f:

$$f^*(y) = \sup_{u \in \mathbf{R}} (yu - f(u)) = \begin{cases} (-y)\log(-y) + (1+y)\log(1+y), & -1 < y < 0 \\ 0 & y = -1 \text{ or } y = 0 \\ \infty, & \text{otherwise.} \end{cases} \tag{13}$$

For general background on convex duality and conjugates, see, *e.g.*, [8, Chap. 5] or [7].

Thus, we have the following Lagrange dual of the ℓ_1-regularized LRP (6):

$$\begin{array}{ll} \text{maximize} & G(\nu) \\ \text{subject to} & \|A^T\nu\|_\infty \le \lambda, \quad b^T\nu = 0, \end{array} \tag{14}$$

where

$$G(\nu) = -(1/m)\sum_{i=1}^m f^*(-m\nu_i) \tag{15}$$

is the dual objective. The dual problem (14) is a convex optimization problem with variable $\nu \in \mathbf{R}^m$, and has the form of an ℓ_∞-norm constrained maximum generalized entropy problem. We say that $\nu \in \mathbf{R}^m$ is *dual feasible* if it satisfies $\|A^T\nu\|_\infty \le \lambda$, $b^T\nu = 0$.

From standard results in convex optimization we have the following.

- *Weak duality.* Any dual feasible point ν gives a lower bound on the optimal value $p^\star$ of the (primal) ℓ_1-regularized LRP (6):

$$G(\nu) \le p^\star. \tag{16}$$

- *Strong duality.* The ℓ_1-regularized LRP (6) satisfies a variation on Slater's constraint qualification, so there is an optimal solution of the dual (14) $\nu^\star$, which satisfies

$$G(\nu^\star) = p^\star.$$

  In other words, the optimal values of the primal (6) and dual (14) are equal.

We can relate a primal optimal point $(v^\star, w^\star)$ and a dual optimal point $\nu^\star$ to the optimality conditions (9) and (10). They are related by

$$\nu^\star = (1/m)(\mathbf{1} - p_{\log}(v^\star, w^\star)). \tag{17}$$

We also note that the dual problem (14) can be derived starting from the equivalent problem (7), by introducing new variables z_i (as we did at (12)), and associating dual variables $\nu_+ \geq 0$ for the inequalities $w \leq u$, and $\nu_- \geq 0$ for the inequalities $-u \leq w$. By identifying $\nu = \nu_+ - \nu_-$ we obtain the dual problem (14).

2.3 Suboptimality bound

We now derive an easily computed bound on the suboptimality of a pair (v, w), by constructing a dual feasible point $\bar{\nu}$ from an arbitrary w. Define $\bar{v}$ as

$$\bar{v} = \arg\min_v l_{\mathrm{avg}}(v, w), \tag{18}$$

i.e., $\bar{v}$ is the optimal intercept for the weight vector w, characterized by $b^T(\mathbf{1}-p_{\log}(\bar{v}, w)) = 0$. Now, we define $\bar{\nu}$ as

$$\bar{\nu} = (s/m)(\mathbf{1} - p_{\log}(\bar{v}, w)), \tag{19}$$

where the scaling constant s is

$$s = \min\left\{m\lambda/\|A^T(\mathbf{1} - p_{\log}(\bar{v}, w))\|_\infty, 1\right\}.$$

Evidently $\bar{\nu}$ is dual feasible, so $G(\bar{\nu})$ is a lower bound on $p^\star$, the optimal value of the ℓ_1-regularized LRP (6).

To compute the lower bound $G(\bar{\nu})$, we first compute $\bar{v}$. This is a one-dimensional smooth convex optimization problem, which can be solved very efficiently, for example, by a bisection method on the optimality condition

$$b^T(\mathbf{1} - p_{\log}(v, w)) = 0,$$

since the lefthand side is a monotone function of v. Newton's method can be used to ensure extremely fast terminal convergence to $\bar{v}$. From $\bar{v}$, we compute $\bar{\nu}$ using (19), and then evaluate the lower bound $G(\bar{\nu})$.

The difference between the primal objective value of (v, w), and the associated lower bound $G(\bar{\nu})$, is called the *duality gap*, and denoted $\eta(v, w)$:

$$\begin{aligned} \eta(v, w) &= l_{\mathrm{avg}}(v, w) + \lambda\|w\|_1 - G(\bar{\nu}) \\ &= (1/m)\textstyle\sum_{i=1}^m \left(f(w^T a_i + v b_i) + f^*(-m\nu_i)\right) + \lambda\|w\|_1. \end{aligned} \tag{20}$$

We always have $\eta(v, w) \geq 0$; and (by weak duality (16)) the point (v, w) is no more than η-suboptimal. At the optimal point $(v^\star, w^\star)$, we have $\eta = 0$.

3 An interior-point method

In this section we describe an interior-point method for solving the ℓ_1-regularized LRP (6), in the equivalent formulation

$$\begin{array}{ll} \text{minimize} & l_{\text{avg}}(v,w) + \lambda \mathbf{1}^T u, \\ \text{subject to} & -u_i \le w_i \le u_i, \quad i = 1, \ldots, n, \end{array} \tag{21}$$

with variables $w, u \in \mathbf{R}^n$ and $v \in \mathbf{R}$.

3.1 Logarithmic barrier and central path

The *logarithmic barrier* for the bound constraints $-u_i \le w_i \le u_i$ is

$$\Phi(w,u) = -\sum_{l=1}^{n} \log(u_i + w_i) - \sum_{l=1}^{n} \log(u_i - w_i) = -\sum_{l=1}^{n} \log(u_i^2 - w_i^2),$$

with domain

$$\mathbf{dom}\, \Phi = \{(w,u) \in \mathbf{R}^n \times \mathbf{R}^n \mid |w_i| < u_i,\ i = 1, \ldots, n\}.$$

The logarithmic barrier function is smooth and convex. We augment the weighted objective function by the logarithmic barrier, to obtain

$$\phi_t(v,w,u) = t l_{\text{avg}}(v,w) + t\lambda \mathbf{1}^T u + \Phi(w,u), \tag{22}$$

where $t > 0$ is a parameter. This function is smooth, strictly convex, and bounded below, and so has a unique minimizer which we denote $(v^\star(t), w^\star(t), u^\star(t))$. This defines a curve in $\mathbf{R} \times \mathbf{R}^n \times \mathbf{R}^n$, parametrized by t, called the *central path*.

With the point $(v^\star(t), w^\star(t), u^\star(t))$ we associate

$$\nu^\star(t) = (1/m)(\mathbf{1} - p_{\log}(v^\star(t), w^\star(t))), \tag{23}$$

which can be shown to be dual feasible. (Indeed, it coincides with the dual feasible point $\bar{\nu}$ constructed from $w^\star(t)$ using the method of §2.3.) The associated duality gap satisfies

$$l_{\text{avg}}(v^\star(t), w^\star(t)) + \lambda \|w^\star(t)\|_1 - G(\nu^\star(t)) \le l_{\text{avg}}(v^\star(t), w^\star(t)) + \lambda \mathbf{1}^T u^\star(t) - G(\nu^\star(t)) = 2n/t.$$

In particular, $(v^\star(t), w^\star(t))$ is no more than $2n/t$-suboptimal, so the central path leads to an optimal solution. (See [8, Chap. 11] for more on the central path.)

In a primal interior-point method, we compute a sequence of points on the central path, for an increasing sequence of values of t, using Newton's method to minimize $\phi_t(v,w,u)$, starting from the previously computed central point. A typical method uses the sequence $t = t_0, \mu t_0, \mu^2 t_0, \ldots$, where μ is between 2 and 50 (see, *e.g.*, [8, §11.3]). The method can be terminated when $2n/t \le \epsilon$, since then we can guarantee ϵ-suboptimality of $(v^\star(t), w^\star(t))$.

3.2 A custom interior-point method

Using our method for cheaply computing a dual feasible point and associated duality gap for *any* (v, w) (and not just for (v, w) on the central path, as in the general case), we can construct a custom interior-point method that updates the parameter t at each iteration.

```
CUSTOM INTERIOR-POINT METHOD FOR $\ell_1$-REGULARIZED LR.
given tolerance $\epsilon > 0$, line search parameters $\alpha \in (0, 1/2)$, $\beta \in (0, 1)$
Set initial values. $t := 1/\lambda$, $v := \log(m_+/m_-)$, $w := 0$, $u := \mathbf{1}$.
repeat
  1. Compute search direction.
       Solve the Newton system $\nabla^2\phi_t(v, w, u) \begin{bmatrix} \Delta v \\ \Delta w \\ \Delta u \end{bmatrix} = -\nabla\phi_t(v, w, u)$.
  2. Backtracking line search. Find the smallest integer $k \geq 0$ that satisfies
       $\phi_t(v + \beta^k\Delta v, w + \beta^k\Delta w, u + \beta^k\Delta u) \leq \phi_t(v, w, u) + \alpha\beta^k\nabla\phi_t(v, w, u)^T \begin{bmatrix} \Delta v \\ \Delta w \\ \Delta u \end{bmatrix}$.
  3. Update. $(v, w, u) := (v, w, u) + \beta^k(\Delta v, \Delta w, \Delta u)$.
  4. Set $v := \bar{v}$, the optimal value of the intercept, as in (18).
  5. Construct dual feasible point $\nu$ from (19).
  6. Evaluate duality gap $\eta$ from (20).
  7. quit if $\eta \leq \epsilon$.
  8. Update $t$.
```

This description is complete, except for the rule for updating the parameter t, which will be described below. Our choice of initial values for v, w, u, and t can be explained as follows. The choice $w = 0$ and $u = \mathbf{1}$ seems to work very well, especially when the original data are standardized. The choice $v = \log(m_+/m_-)$ is the optimal value of v when $w = 0$ and $u = \mathbf{1}$, and the choice $t = 1/\lambda$ minimizes $\|(1/t)\nabla\phi_t(\log(m_+/m_-), 0, \mathbf{1})\|_2$. (In any case, the choice of the initial values does not greatly affect performance.) The construction of a dual feasible point and duality gap, in steps 4–6, is explained in §2.3. Typical values for the line search parameters are $\alpha = 0.01$, $\beta = 0.5$, but here too, these parameter values do not have a large effect on performance. The computational effort per iteration is dominated by step 1, the search direction computation.

There are many possible update rules for the parameter t. In a classical primal barrier method, t is held constant until ϕ_t is (approximately) minimized, *i.e.*, $\|\nabla\phi_t\|_2$ is small; when this occurs, t is increased by a factor typically between 2 and 50. More sophisticated update rules can be found in, *e.g.*, [38, 58, 59].

The update rule we propose is

$$t := \begin{cases} \max\left\{\mu \min\{\hat{t}, t\}, t\right\}, & s \geq s_{\min} \\ t, & s < s_{\min} \end{cases} \tag{24}$$

where $\hat{t} = 2n/\eta$, and $s = \beta^k$ is the step length chosen in the line search. Here $\mu > 1$ and $s_{\min} \in (0, 1]$ are algorithm parameters; we have found good performance with $\mu = 2$ and $s_{\min} = 0.5$.

To explain the update rule (24), we first give an interpretation of $\hat{t}$. If (v, w, u) is on the central path, *i.e.*, ϕ_t is minimized, the duality gap is $\eta = 2n/t$. Thus $\hat{t}$ is the value of t for which the associated central point has the same duality gap as the current point. Another interpretation is that if t were held constant at $t = \hat{t}$, (v, w, u) would converge to $(v^\star(\hat{t}), w^\star(\hat{t}), u^\star(\hat{t}))$, at which point the duality gap would be exactly η.

We use the step length s as a crude measure of proximity to the central path. When the current point is near the central path, *i.e.*, ϕ_t is nearly minimized, we have $s = 1$; far from the central path, we typically have $s \ll 1$. Now we can explain the update rule (24). When the current point is near the central path, as judged by $s \geq s_{\min}$ and $\hat{t} \approx t$, we increase t by a factor μ; otherwise, we keep t at its current value.

We can give an informal justification of convergence of the custom interior-point algorithm. (A formal proof of convergence would be quite long.) Assume that the algorithm does not terminate. Since t never decreases, it either increases without bound, or converges to some value $\bar{t}$. In the first case, the duality gap η converges to zero, so the algorithm must exit. In the second case, the algorithm reduces (roughly) to Newton's method for minimizing $\phi_{\bar{t}}$. This must converge, which means that (v, w, u) converges to $(v^\star(\bar{t}), w^\star(\bar{t}), u^\star(\bar{t}))$. Therefore the duality gap converges to $\bar{\eta} = 2n/\bar{t}$. A basic property of Newton's method is that near the solution, the step length is one. At the limit, we therefore have

$$\bar{t} = \max\left\{\mu \min\{2n/\bar{\eta}, \bar{t}\}, \bar{t}\right\} = \mu\bar{t},$$

which is a contradiction since $\mu > 1$.

3.3 Gradient and Hessian

In this section we give explicit formulas for the gradient and Hessian of ϕ_t. The gradient $g = \nabla\phi_t(v, w, u)$ is given by

$$g = \begin{bmatrix} g_1 \\ g_2 \\ g_3 \end{bmatrix} \in \mathbf{R}^{2n+1},$$

where

$$\begin{aligned} g_1 &= \nabla_v \phi_t(v,w,u) = -(t/m) b^T (\mathbf{1} - p_{\log}(v,w)) \in \mathbf{R}, \\ g_2 &= \nabla_w \phi_t(v,w,u) = -(t/m) A^T (\mathbf{1} - p_{\log}(v,w)) + \left[\begin{array}{c} 2w_1/(u_1^2 - w_1^2) \\ \vdots \\ 2w_n/(u_n^2 - w_n^2) \end{array}\right] \in \mathbf{R}^n, \\ g_3 &= \nabla_u \phi_t(v,w,u) = t\lambda \mathbf{1} - \left[\begin{array}{c} 2u_1/(u_1^2 - w_1^2) \\ \vdots \\ 2u_n/(u_n^2 - w_n^2) \end{array}\right] \in \mathbf{R}^n. \end{aligned}$$

The Hessian $H = \nabla^2 \phi_t(v,w,u)$ is given by

$$H = \left[\begin{array}{ccc} tb^T D_0 b & tb^T D_0 A & 0 \\ tA^T D_0 b & tA^T D_0 A + D_1 & D_2 \\ 0 & D_2 & D_1 \end{array}\right] \in \mathbf{R}^{(2n+1)\times(2n+1)},$$

where

$$\begin{aligned} D_0 &= (1/m)\,\mathbf{diag}(f''(w^T a_1 + v b_1), \ldots, f''(w^T a_m + v b_m)), \\ D_1 &= \mathbf{diag}\left(2(u_1^2 + w_1^2)/(u_1^2 - w_1^2)^2, \ldots, 2(u_n^2 + w_n^2)/(u_n^2 - w_n^2)^2\right), \\ D_2 &= \mathbf{diag}\left(-4u_1 w_1/(u_1^2 - w_1^2)^2, \ldots, -4u_n w_n/(u_n^2 - w_n^2)^2\right). \end{aligned}$$

Here, we use $\mathbf{diag}(z_1, \ldots, z_m)$ to denote the diagonal matrix with diagonal entries $z_1, \ldots, z_m$, where $z_i \in \mathbf{R}$, $i = 1, \ldots, m$. The Hessian H is symmetric and positive definite.

3.4 Computing the search direction

The search direction is defined by the linear equations (Newton system)

$$\left[\begin{array}{ccc} tb^T D_0 b & tb^T D_0 A & 0 \\ tA^T D_0 b & tA^T D_0 A + D_1 & D_2 \\ 0 & D_2 & D_1 \end{array}\right] \left[\begin{array}{c} \Delta v \\ \Delta w \\ \Delta u \end{array}\right] = - \left[\begin{array}{c} g_1 \\ g_2 \\ g_3 \end{array}\right]. \qquad (25)$$

We first eliminate Δu to obtain the reduced Newton system

$$H_{\text{red}} \left[\begin{array}{c} \Delta v \\ \Delta w \end{array}\right] = -g_{\text{red}}, \qquad (26)$$

where

$$H_{\text{red}} = \left[\begin{array}{cc} tb^T D_0 b & tb^T D_0 A \\ tA^T D_0 b & tA^T D_0 A + D_3 \end{array}\right], \quad g_{\text{red}} = \left[\begin{array}{c} g_1 \\ g_2 - D_2 D_1^{-1} g_3 \end{array}\right], \quad D_3 = D_1 - D_2 D_1^{-1} D_2.$$

Once this reduced system is solved, Δu can be recovered as

$$\Delta u = -D_1^{-1}(g_3 + D_2 \Delta w).$$

Several methods can be used to solve the reduced Newton system (26), depending on the relative sizes of n and m and the sparsity of the data A.

More examples than features

We first consider the case when $m \geq n$, *i.e.*, there are more examples than features. We form H_{red}, at a cost of $O(mn^2)$ flops (floating-point operations), then solve the reduced system (26) by Cholesky factorization of H_{red}, followed by back and forward substitution steps, at a cost of $O(n^3)$ flops. The total cost using this method is $O(mn^2 + n^3)$ flops, which is the same as $O(mn^2)$ when there are more examples than features.

When A is sufficiently sparse, the matrix $tA^T D_0 A + D_3$ is sparse, so H_{red} is sparse, with a dense first row and column. By exploiting sparsity in forming $tA^T D_0 A + D_3$, and using a sparse Cholesky factorization to factor H_{red}, the complexity can be much smaller than $O(mn^2)$ flops (see [8, §C], [23, 3]).

Fewer examples than features

When $m \leq n$, *i.e.*, there are fewer examples than features, the matrix H_{red} is a diagonal matrix plus a rank $m+1$ matrix, so we can use the Sherman-Morrison-Woodbury formula to solve the reduced Newton system (26) at a cost of $O(m^2 n)$ flops (see, *e.g.*, [8, §C.4.3]). We start by eliminating Δw from (26) to obtain

$$(tb^T D_0 b - t^2 b^T D_0 A S^{-1} A^T D_0 b)\Delta v = -g_1 + tb^T D_0 A S^{-1}(g_2 - D_2 D_1^{-1} g_3), \qquad (27)$$

where $S = tA^T D_0 A + D_3$. By the Sherman-Morrison-Woodbury formula, the inverse of S is given by

$$S^{-1} = D_3^{-1} - D_3^{-1} A^T \left((1/t)D_0^{-1} + A D_3^{-1} A^T\right)^{-1} A D_3^{-1}. \qquad (28)$$

We can now calculate Δv via Cholesky factorization of the matrix $\left((1/t)D_0^{-1} + A D_3^{-1} A^T\right)$ and two backsubstitutions. Once we compute Δv, we can compute the other components of the search direction as

$$\begin{aligned} \Delta w &= -S^{-1}(g_2 - D_2 D_1^{-1} g_3 + tA^T D_0 b \Delta v), \\ \Delta u &= -D_1^{-1}(g_3 + D_2 \Delta w). \end{aligned}$$

The total cost of computing the search direction is $O(m^2 n)$ flops. We can exploit sparsity in the Cholesky factorization, whenever $(1/t)D_0^{-1} + A D_3^{-1} A^T$ is sufficiently sparse, to reduce the complexity.

Summary

In summary, the number of flops needed to compute the search direction is

$$O(\min(n,m)^2 \max(n,m)),$$

using dense matrix methods. If $m \geq n$ and $A^T A$ is sparse, or $m \leq n$ and AA^T is sparse, we can use (direct) sparse matrix methods to compute the search direction with less effort. In each of these cases, the computational effort per iteration of the interior-point method is the same as the effort of solving one ℓ_2-regularized linear regression problem.

Data	Features n	Examples m	$\lambda/\lambda_{\max}$	card(w)	IP iterations	Time (sec)
Leukemia [25]	7129	38	0.5	6	37	1.38
			0.1	14	38	1.30
			0.05	14	39	1.34
Colon [2]	2000	62	0.5	7	35	0.58
			0.1	22	32	0.53
			0.05	25	33	0.55
Adult [39]	14	30162	0.5	2	29	3.50
			0.1	8	30	4.21
			0.05	9	30	3.95
Spambase [39]	57	4061	0.5	8	31	1.17
			0.1	28	32	1.21
			0.05	38	33	1.32

Table 1: Performance of interior-point method on 4 data sets, each for 3 values of λ.

4 Numerical examples

In this section we give some numerical examples to illustrate the performance of the interior-point method described in §3, using algorithm parameters

$$\alpha = 0.01, \qquad \beta = 0.5, \qquad s_{\min} = 0.5, \qquad \gamma = 2, \qquad \epsilon = 10^{-8}.$$

(The algorithm performs well for much smaller values of ϵ, but this accuracy is more than adequate for any practical use.) The algorithm was implemented in Matlab, and run on a 3.2GHz Pentium IV under Linux.

4.1 Benchmark problems

The data are four small standard data sets taken from the UCI machine learning benchmark repository [39] and other sources. The first data set is leukemia cancer gene expression data [25], the second is colon tumor gene expression data [2], the third is adult (census income) data [39], and the fourth is spambase data [39]. For each data set, we considered three values of the regularization parameter: $\lambda = 0.5\lambda_{\max}$, $\lambda = 0.1\lambda_{\max}$, and $\lambda = 0.05\lambda_{\max}$. We discarded examples with missing data (in the adult data set), and standardized each data set. The dimensions of each problem, along with the number of interior-point method iterations needed, and the execution time, are given in table 1. In reporting card(w), we consider a component w_i to be zero when $|w_i| < 10^{-4}\|w\|_2/\sqrt{n}$.

In all twelve examples, around 35 iterations were required. We have observed this behavior over a large number of other examples as well. The execution times are well predicted by the complexity order $\min(m,n)^2 \max(m,n)$, with the exception of the Adult data, where n is so small that operations of order m are siginificant compared to those of order mn^2.

Figure 1 shows the progress of the interior-point method on the four data sets, for the same three values of λ. The vertical axis shows duality gap, and the horizontal axis shows

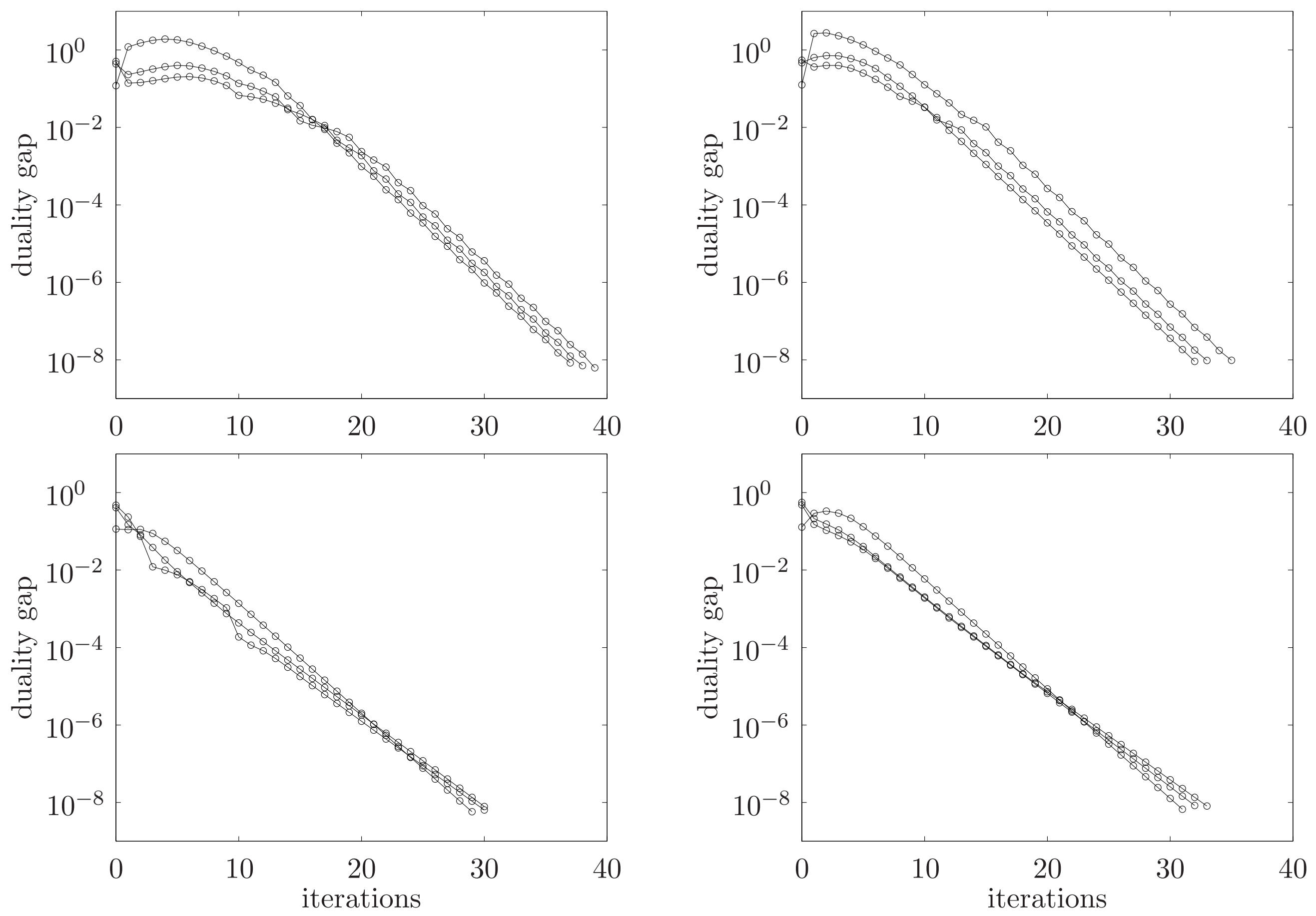

Figure 1: Progress of the interior-point method on 4 data sets, showing duality gap versus iteration number. *Top left*: Leukemia cancer gene data set. *Top right*: Colon tumor gene data set. *Bottom left*: Adult data set. *Bottom right*: Spambase data set.

iteration number, which is the natural measure of computational effort when dense linear algebra methods are used. The figures show that the algorithm has linear convergence, with duality gap decreasing by a factor around 1.85 in each iteration.

4.2 Randomly generated problems

To examine the effect of problem size on the number of iterations required, we generate 100 random problem instances for each of 20 values of n, ranging from $n = 100$ to $n = 10000$, with $m = 0.1n$, *i.e.*, 10 times more features than examples. Each problem has an equal number of positive and negative examples, *i.e.*, $m_+ = m_- = m/2$. Features of positive (negative) examples are independent and identically distributed, drawn from a normal distribution $\mathcal{N}(v, 1)$, where v is in turn drawn from a uniform distribution on $[0, 1]$ ($[-1, 0]$).

For each of the 2000 data sets, we solve the ℓ_1-regularized LRP for $\lambda = 0.5\lambda_{\max}$, $\lambda = 0.1\lambda_{\max}$, and $\lambda = 0.05\lambda_{\max}$. The lefthand plot in figure 2 shows the mean and standard

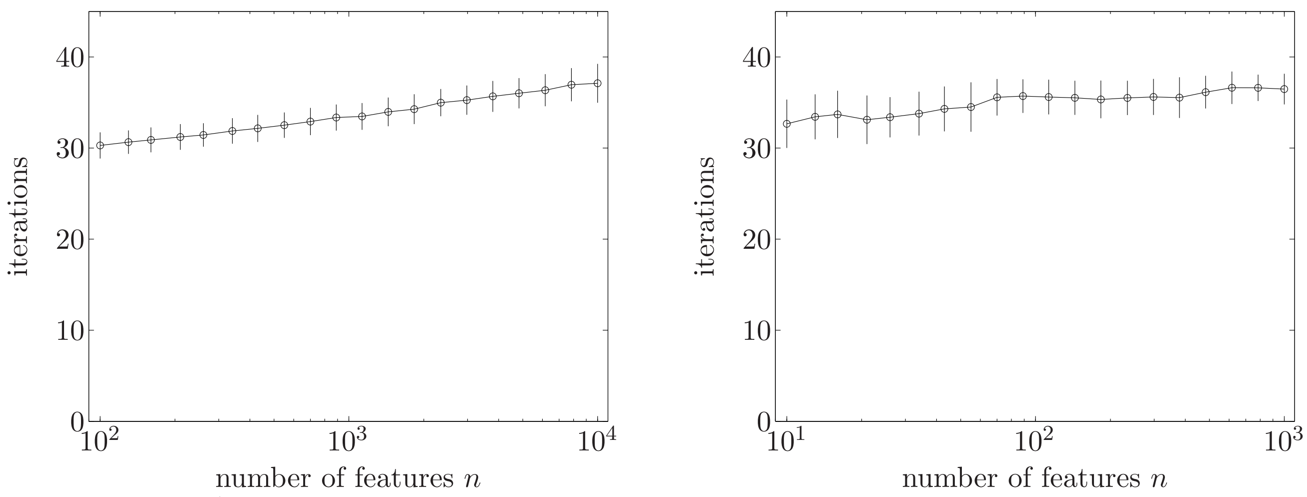

Figure 2: Average number of iterations required to solve 100 randomly generated ℓ_1-regularized LRPs with different problem size and regularization parameter. *Left:* $n = 10m$. *Right:* $n = 0.1m$. Error bars show standard deviation.

deviation of the number of iterations required to solve the 100 problem instances associated with each value of n and λ. It can be seen that the number of iterations required is very near 35, for all 6000 problem instances.

In the same way, we generate a family of data sets with $m = 10n$, *i.e.*, 10 times more examples than features, with 100 problem instances for each of 20 values of n ranging from $n = 10$ to $n = 1000$, and for the same 3 values of λ. The righthand plot in figure 2 shows the mean and standard deviation of the number of iterations required to solve the 100 problem instances associated with each value of n and λ. The results are quite similar to the case with $m = 0.1n$.

5 Truncated Newton interior-point method

In this section we describe a variation on our interior-point method that can handle very large problems, provided the data matrix A is sparse, at the cost of having a run time that is less predictable. The basic idea is to compute the search direction approximately, using a preconditioned conjugate gradients (PCG) method. When the search direction in Newton's method is computed approximately, using an iterative method such as PCG, the overall algorithm is called a *conjugate gradient Newton method*, or a *truncated Newton method* [48, 16]. Truncated Newton methods have been applied to interior-point methods; see, *e.g.*, [55, 45].

5.1 Preconditioned conjugate gradients

The PCG algorithm [17, §6.6] computes an approximate solution of the linear equations $Hx = -g$, where $H \in \mathbf{R}^{N\times N}$ is symmetric positive definite. It uses a preconditioner $P \in \mathbf{R}^{N\times N}$, also symmetric positive definite.

Preconditioned Conjugate Gradients Algorithm

```
given relative tolerance $\epsilon_{\rm pcg} > 0$, iteration limit $N_{\rm pcg}$, and $x_0 \in \mathbf{R}^k$
$k := 0$, $r_0 := Hx_0 - g$, $p_1 := -P^{-1}g$, $y_0 := P^{-1}r_0$.
repeat
    $k := k+1$
    $z := Hp_k$
    $\nu_k := y_{k-1}^T r_{k-1}/p_k^T z$
    $x_k := x_{k-1} + \nu_k p_k$
    $r_k := r_{k-1} - \nu_k z$
    $y_k := P^{-1}r_k$
    $\mu_{k+1} := y_k^T r_k / y_{k-1}^T r_{k-1}$
    $p_{k+1} := y_k + \mu_{k+1} p_k$
until $\|r_k\|_2/\|g\|_2 \le \epsilon_{\rm pcg}$ or $k = N_{\rm pcg}$.
```

Each iteration of the PCG algorithm involves a handful of inner products, the matrix-vector product Hp_k and a solve step with P in computing $P^{-1}r_k$. With exact arithmetic, and ignoring the stopping condition, the PCG algorithm is guaranteed to compute the exact solution $x = -H^{-1}g$ in N steps. When $P^{-1/2}HP^{-1/2}$ is well conditioned, or has just a few extreme eigenvalues, the PCG algorithm can compute an approximate solution in a number of steps that can be far smaller than N. Since $P^{-1}r_k$ is computed in each step, we need this computation to be efficient.

5.2 Truncated Newton interior-point method

The truncated Newton interior-point method is the same as the interior-point algorithm described in §3, with the search direction computed using the PCG algorithm.

We can compute Hp_k in the PCG algorithm using

$$\begin{aligned} Hp_k &= \begin{bmatrix} tb^TD_0b & tb^TD_0A & 0 \\ tA^TD_0b & tA^TD_0A + D_1 & D_2 \\ 0 & D_2 & D_1 \end{bmatrix} \begin{bmatrix} p_{k1} \\ p_{k2} \\ p_{k3} \end{bmatrix} \\ &= \begin{bmatrix} b^Tu \\ A^Tu + D_1p_{k2} \\ D_2p_{k2} + D_1p_{k3} \end{bmatrix}, \end{aligned}$$

where $u = tD_0(bp_{k1} + Ap_{k2}) \in \mathbf{R}^m$. The cost of computing Hp_k is $O(p)$ flops when A is sparse with p nonzero elements. (We assume $p \geq n$, which holds if each example has at least one nonzero feature.)

We now describe a simple choice for the preconditioner P. The Hessian can be written as

$$H = t\nabla^2 l_{\rm avg}(v, w) + \nabla^2 \Phi(w, u).$$

To obtain the preconditioner, we replace the first term with its diagonal part, to get

$$P = \mathrm{diag}\left(t\nabla^2 l_{\rm avg}(v, w)\right) + \nabla^2 \Phi(w, u) = \begin{bmatrix} d_0 & 0 & 0 \\ 0 & D_4 & D_2 \\ 0 & D_2 & D_1 \end{bmatrix}, \qquad (29)$$

where

$$d_0 = tb^T D_0 b, \qquad D_4 = \mathrm{diag}(tA^T D_0 A) + D_1.$$

(Here $\mathrm{diag}(S)$ is the diagonal matrix obtained by setting the off-diagonal entries of the matrix S to zero.) This preconditioner approximates the Hessian of $tl_{\rm avg}$ with its diagonal entries, while retaining the Hessian of the logarithmic barrier. For this preconditioner, $P^{-1}r_k$ can be computed cheaply as

$$\begin{aligned} P^{-1}r_k &= \begin{bmatrix} d_0 & 0 & 0 \\ 0 & D_3 & D_2 \\ 0 & D_2 & D_1 \end{bmatrix}^{-1} \begin{bmatrix} r_{k1} \\ r_{k2} \\ r_{k3} \end{bmatrix} \\ &= \begin{bmatrix} r_{k1}/d_0 \\ (D_1 D_3 - D_2^2)^{-1}(D_1 r_{k2} - D_2 r_{k3}) \\ (D_1 D_3 - D_2^2)^{-1}(-D_2 r_{k2} + D_3 r_{k3}) \end{bmatrix}, \end{aligned}$$

which requires $O(n)$ flops.

We can now explain how *implicit standardization* can be carried out. When using standardized data, we work with the matrix $A^{\rm std}$ defined in (8), instead of A. As mentioned in §1.5, $A^{\rm std}$ is in general dense, so we should not form the matrix. In the truncated Newton interior-point method we do not need to form the matrix $A^{\rm std}$; we only need a method for multiplying a vector by $A^{\rm std}$ and a method for multiplying a vector by $A^{{\rm std}\,T}$. But this is easily done efficiently, using the fact that $A^{\rm std}$ is a sparse matrix (*i.e.*, A) times a diagonal matrix, plus a rank-one matrix (see (8)).

There are several good choices for the initial point in the PCG algorithm (labeled x_0 in §5.1), such as the negative gradient, or the previous search direction. We have found good performance with both, with a small advantage in using the previous search direction.

The PCG relative tolerance parameter $\epsilon_{\rm pcg}$ has to be carefully chosen to obtain good efficiency in a truncated Newton method. If the tolerance is too small, too many PCG steps are need to compute each search direction; if the tolerance is too high, then the computed search directions do not give adequate reduction in duality gap per iteration. We experimented with several methods of adjusting the PCG relative tolerance, and found good results with the adaptive rule

$$\epsilon_{\mathrm{pcg}} = \min\left\{0.1, \eta/\|g\|_2\right\}, \tag{30}$$

where g is the gradient and η is the duality gap at the current iterate. Thus, we solve the Newton system with low accuracy (but never worse than 10%) at early iterations, and solve it more accurately as the duality gap decreases. This adaptive rule is similar in spirit to standard methods used in inexact and truncated Newton methods; see, *e.g.*, [41].

The computational effort of the truncated Newton interior-point algorithm is the product of s, the total number of PCG steps required over all iterations, and the cost of a PCG step, which is $O(p)$, where p is the number of nonzero entries in A, *i.e.*, the total number of (nonzero) features appearing in all examples. In extensive testing, we found the truncated Newton interior-point method to be very efficient, requiring a total number of PCG steps ranging between a few hundred (for medium size problems) and several thousand (for large problems). For medium size (and sparse) problems it was faster than the basic interior-point method; moreover the truncated Newton interior-point method was able to solve very large problems, for which forming the Hessian H (let alone computing the search direction) would be prohibitively expensive.

While the total number of iterations in the basic interior-point method is around 35, and nearly independent of the problem size and problem data, the total number of PCG iterations required by the truncated Newton interior-point method can vary significantly with problem data and the value of the regularization parameter λ. In particular, for small values of λ (which lead to large values of $\mathrm{card}(w)$), the truncated Newton interior-point method requires a larger total number of PCG steps. Algorithm performance that depends substantially on problem data, as well as problem dimension, is typical of all iterative (*i.e.*, non direct) methods, and is the price paid for the ability to solve very large problems.

5.3 Numerical examples

In this section we give some numerical examples to illustrate the performance of the truncated Newton interior-point method. We use the same algorithm parameters for line search, update rule, and stopping criterion as those used in §4, and the PCG tolerance given in (30). We chose the parameter N_{pcg} to be large enough (1000) that the iteration limit was never reached in our experiments; the typical number of PCG iterations was far smaller. The algorithm is implemented in Matlab, on a 3.2GHz Pentium IV running Linux.

A small problem

We consider the leukemia cancer gene expression data set, with $\lambda = 0.5\lambda_{\max}$, $\lambda = 0.1\lambda_{\max}$, and $\lambda = 0.05\lambda_{\max}$, exactly as in §4.1. Figure 3 shows the convergence behavior. The lefthand plot shows the duality gap versus outer iterations; the lefthand plot shows duality gap versus cumulative PCG iterations, which is the more accurate measure of computational effort.

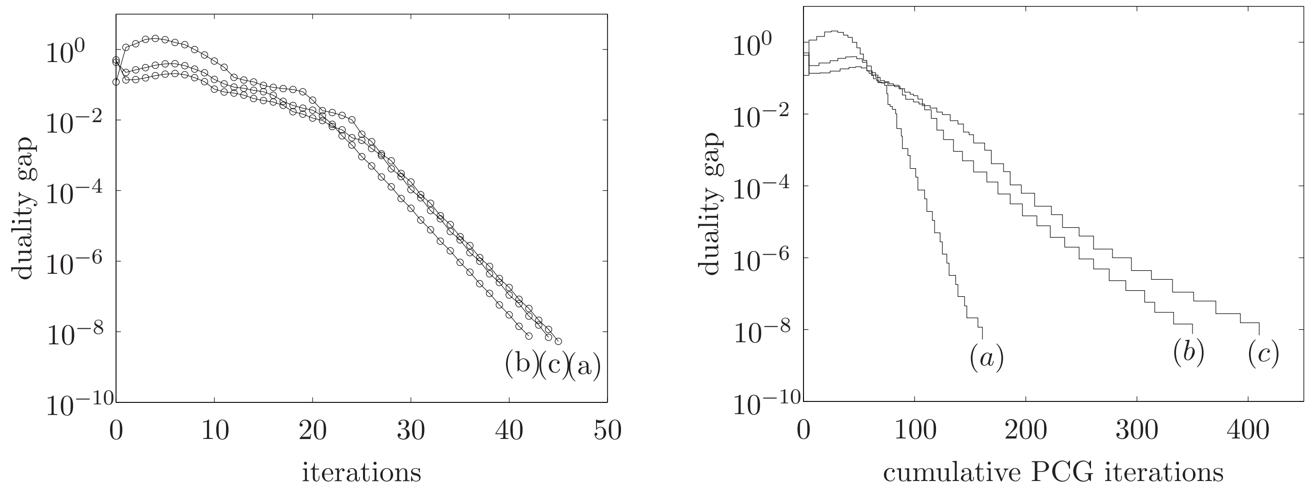

Figure 3: Progress of the truncated Newton interior-point method on the leukemia data set with three regularization parameters: (a) $\lambda = 0.5\lambda_{\max}$, (b) $\lambda = 0.1\lambda_{\max}$, and (c) $\lambda = 0.05\lambda_{\max}$.

The lefthand plot shows that the number of Newton iterations required to solve the problem is not much more than in the basic interior-point method. The righthand plot shows that the total number of PCG steps is several hundred, and depends substantially on the value of λ. Thus, the search directions are computed using on the order of ten (or fewer) PCG iterations. To give a very rough comparison with the direct method, we note that a single PCG iteration costs $O(mn)$, whereas a single iteration of the basic interior-point method costs $O(m^2n)$. Since $m = 38$, the several hundred PCG steps are (very roughly) equivalent to around 10 iterations of the basic interior-point method, which suggests that the truncated Newton interior-point method should be comparable to, or perhaps a bit faster than, the basic interior-point method. In fact, the elapsed time for the truncated Newton interior-point method is around twice the time required by the basic interior-point method, but this includes a large overhead since in our implementation, the PCG algorithm is interpreted.

A large problem

Our next example uses the 20 Newsgroups data set [33]. We processed the data set in a way similar to [29]. The positive class consists of the 10 groups with names of form sci.*, comp.*, and misc.forsale, and the negative class consists of the other 10 groups. We used McCallum's Rainbow program [35] with the command

```
    rainbow -g 3 -h -s -O 2 -i
```

to tokenize the (text) data set. These options specify trigrams, skip message headers, no stoplist, and drop terms occurring fewer than two times. The resulting data set has $n = 777811$ features (trigrams) and $m = 11314$ examples (articles). Each example contains an

$\lambda/\lambda_{\max}$	card(w)	Iterations	PCG iterations	Time (min)
0.5	7	56	312	10
0.1	531	75	715	21
0.05	2495	86	1638	46

Table 2: Performance of truncated Newton interior-point method on the 20 Newsgroup data set ($n = 777811$ features, $m = 11314$ examples) for 3 values of λ.

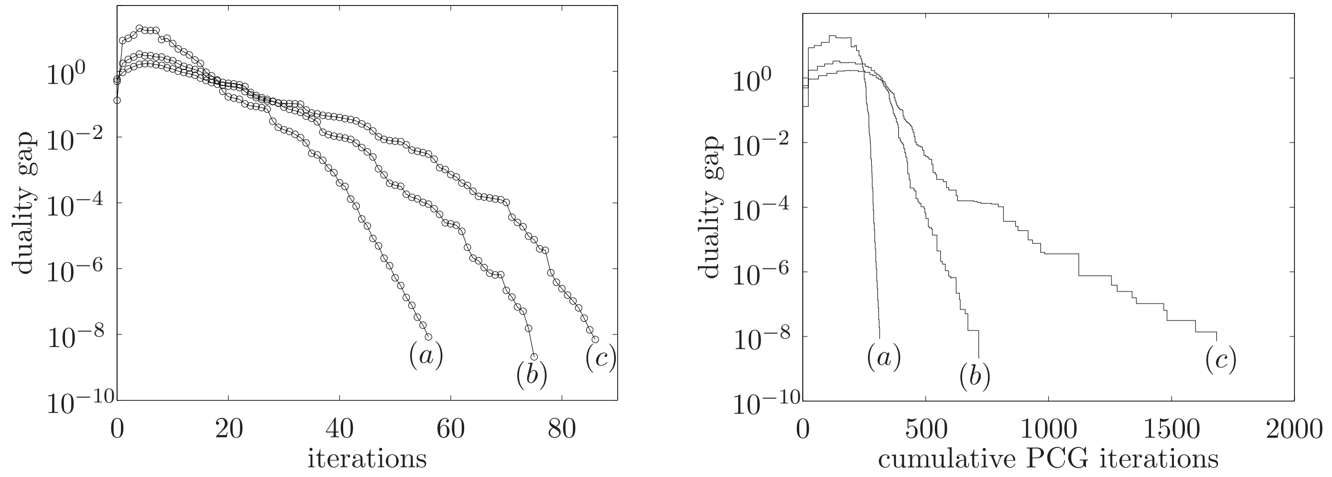

Figure 4: Progress of the truncated Newton interior-point method on the 20 Newsgroups data set for (a) $\lambda = 0.5\lambda_{\max}$, (b) $\lambda = 0.1\lambda_{\max}$, and (c) $\lambda = 0.05\lambda_{\max}$. *Left.* Duality gap versus iterations. *Right.* Duality gap versus cumulative PCG iterations.

average of 425 nonzero features. The total number of nonzero entries in the data matrix A is $p = 4802169$. We standardized the data set using implicit standardization, as explained in §5.2, solving three ℓ_1-regularized LRPs, with $\lambda = 0.5\lambda_{\max}$, $\lambda = 0.1\lambda_{\max}$, and $\lambda = 0.05\lambda_{\max}$. The performance of the algorithm, and the cardinality of the weight vectors, is given in table 2. Figure 4 shows the progress of the algorithm, with duality gap versus iteration (lefthand plot), and duality gap versus cumulative PCG iteration (righthand plot).

The number of iterations required to solve the problems ranges between 56 and 86, depending on λ. The more relevant measure of computational effort is the total number of PCG iterations, which ranges between around 300 and 1600, again, increasing with decreasing λ, which corresponds to increasing card(w). The average number of PCG iterations, per iteration of the truncated Newton interior-point method, is around 5.6 for $\lambda = 0.5\lambda_{\max}$, 9.5 for $\lambda = 0.1\lambda_{\max}$, and 19 for $\lambda = 0.05\lambda_{\max}$. (The variance in the number of PCG iterations required per iteration, however, is large.) The running time is consistent with a cost of around 1.5 seconds per PCG iteration. The increase in running time, for decreasing λ, is due primarily to an increase in the average number of PCG iterations required per iteration, but also siginificantly from an increase in the overall number of iterations required.

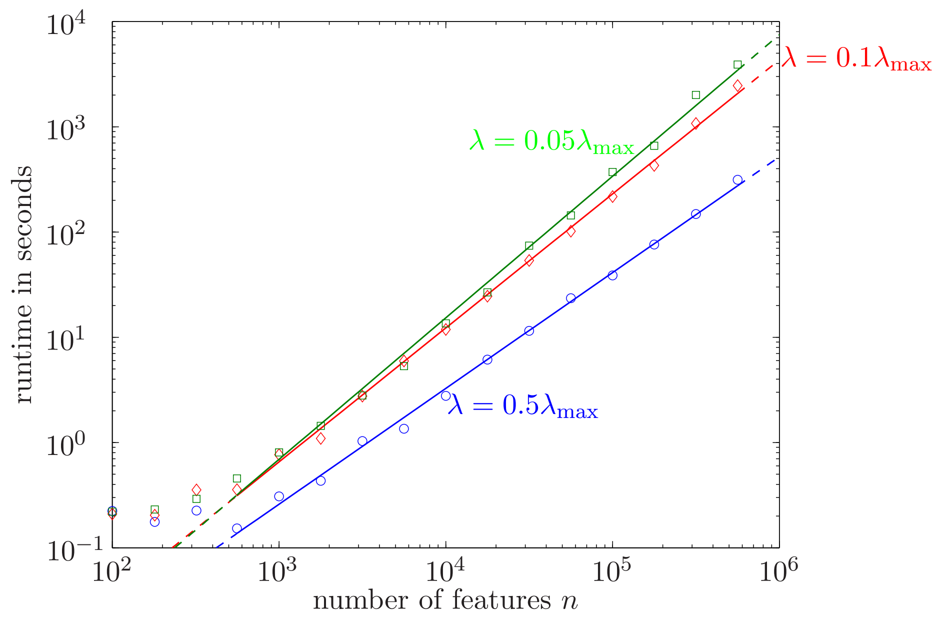

Figure 5: Runtime of the truncated Newton interior-point method, for randomly generated sparse problems, with three values of λ.

Randomly generated problems

We generated a family of 16 data sets, with the number of features n varying from one hundred to one million, and $m = 0.1n$ examples. The data were generated using the same general method described in §4.2, but with A sparse, with an average number of nonzero features per example around 20. Thus, the total number of nonzero entries in A is $p \approx 20n$. We solved each problem instance for the three values $\lambda = 0.5\lambda_{\max}$, $\lambda = 0.1\lambda_{\max}$, and $\lambda = 0.05\lambda_{\max}$. The total runtime, for the 48 ℓ_1-regularized LRPs, is shown in figure 5. The plot shows that runtime increases as λ decreases, and grows approximately linearly with problem size.

We compared the runtimes of the truncated Newton interior-point and the basic interior-point method, using both dense linear algebra methods, and sparse linear algebra methods, to compute the search direction. Figure 6 shows the results for $\lambda = 0.5\lambda_{\max}$. Evidently the truncated Newton interior-point method is more efficient for small problems, and far more efficient for medium problems. For large problems, the basic interior-point method fails due to memory limitations, or extremely long computation times.

By fitting an exponent to the data over the range from $n = 400$ to the largest problem successfully solved by each method, we find that the basic interior-point method scales as $O(n^{2.7})$ (which is consistent with the basic flop count analysis, which predicts $O(n^3)$). When sparse matrix methods are used to compute the search direction in the basic interior-point method, we get an empirical complexity of $O(n^{2.2})$, showing a good efficiency gain over dense methods, for medium scale problems. For the truncated Newton interior-point method, the empirical complexity is $O(n^{1.1})$, *i.e.*, the runtime increases almost linearly with problem size.

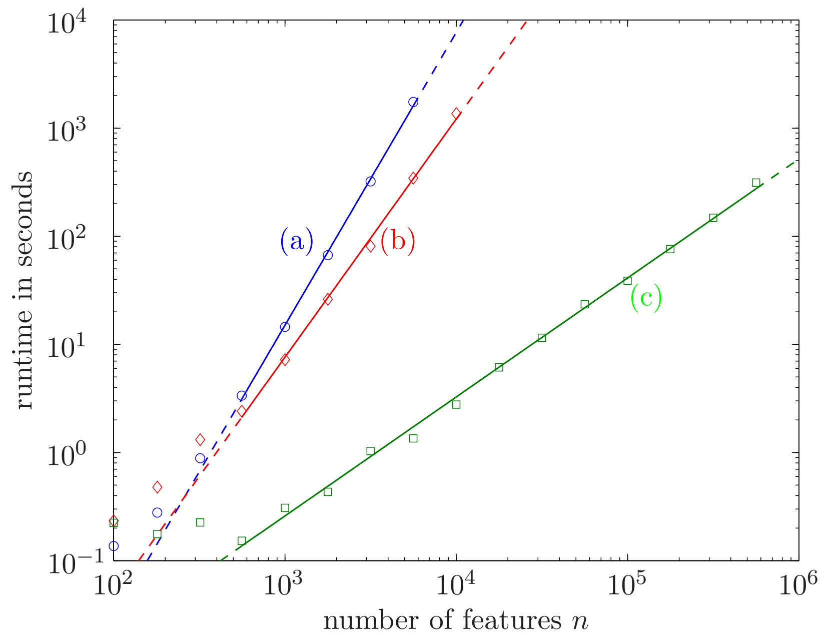

Figure 6: Runtime of (a) basic interior-point method, (b) basic interior-point method with sparse search direction computation, and (c) truncated Newton interior-point method, for a family of randomly generated sparse problems.

Preconditioner performance

To examine the effect of the preconditioner (29) on the efficiency of the approximate search direction computation, we compare the eigenvalue distributions of the Hessian H and the preconditioned Hessian $P^{-1/2}HP^{-1/2}$, for the colon gene tumor problem ($n = 2000$ features, $m = 62$ examples) at the 15th iterate, in figure 7. The eigenvalues of the preconditioned Hessian are tightly clustered, with just a few extreme eigenvalues, which explains the good performance with relatively few PCG iterations per iteration [17, §6.6.5].

6 Computing the regularization path

In this section we consider the problem of solving the ℓ_1-regularized LRP for M values of the regularization parameter λ,

$$\lambda_{\max} = \lambda_1 > \lambda_2 > \cdots > \lambda_M > 0.$$

This can be done by applying the methods described above, for each of the M problems. This is called a *cold-start* approach, since each problem is solved independently of the others. This is efficient when multiple processors are used, since the LRPs can be solved simultaneously, on different processors. But when one processor is used, we can solve these M problems much more efficiently by solving them sequentially, using the previously computed solution as a starting point for the next computation. This is called a *warm-start* approach.

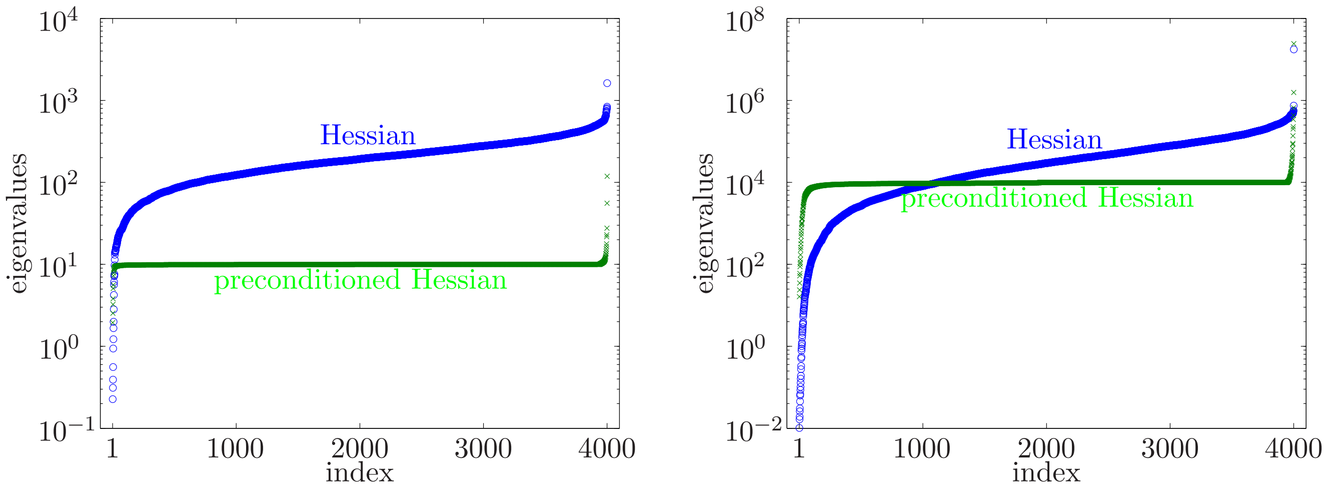

Figure 7: Eigenvalue distributions of Hessian and preconditionned Hessian, at the 15th iterate, for the colon gene tumor problem, for $\lambda = 0.5\lambda_{\max}$ (left) and $\lambda = 0.05\lambda_{\max}$ (right).

We first note that the solution for $\lambda = \lambda_1 = \lambda_{\max}$ is $(\log(m_+/m_-), 0, 0)$. Since this point does not satisfy $|w_i| < u_i$, it cannot be used to initialize the computation for $\lambda = \lambda_2$. We modify it by adding a small increment to u to get

$$(v^{(1)}, w^{(1)}, u^{(1)}) = (\log(m_+/m_-), 0, (\epsilon_{\text{abs}}/(n\lambda))\mathbf{1}),$$

which is strictly feasible. In fact, it is on the central path with parameter $t = 2n/\epsilon_{\text{abs}}$, and so is ϵ_{abs}-suboptimal. Note that so far we have expended no computational effort.

Now for $k = 2, \ldots, M$ we compute the solution $(v^{(k)}, w^{(k)}, u^{(k)})$ of the problem with $\lambda = \lambda_k$, by applying the interior-point method, with starting point modified to be

$$(v_{\text{init}}, w_{\text{init}}, u_{\text{init}}) = (v^{(k-1)}, w^{(k-1)}, u^{(k-1)}),$$

and initial value of t set to $t = 2\zeta n/\epsilon_{\text{abs}}$ where $\zeta \in (0, 1)$ is an algorithm parameter. We have found that $\zeta = 0.9$ works well for a wide range of problems.

6.1 Numerical results

Our first example is the leukemia cancer gene expression data, for $M = 100$ values of λ, uniformly distributed on a logarithmic scale over the interval $[0.01\lambda_{\max}, \lambda_{\max}]$. (For this example, $\lambda_{\max} = 0.37$.) The left plot in figure 8 shows the regularization path, *i.e.*, $w^{(k)}$, versus regularization parameter λ. The right plot shows the number of iterations required to solve each problem from a warm-start, and from a cold-start.

The number of cold-start iterations required is always near 37, while the number of warm-start iterations varies, but is always smaller, and typically much smaller, with an average value of 3.5. Thus the computational savings for this example is over 10 : 1.

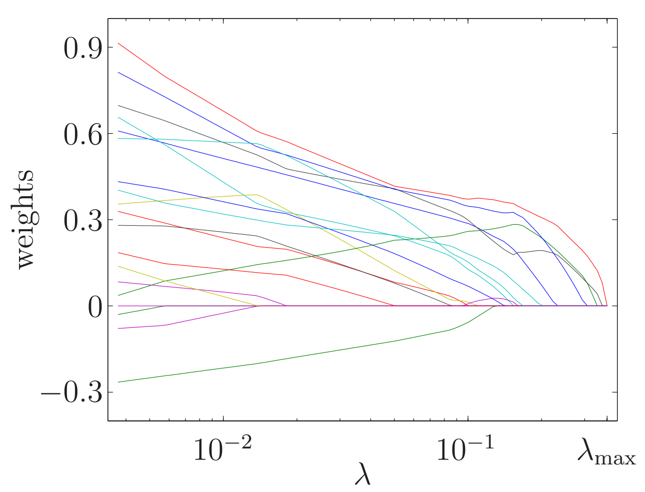

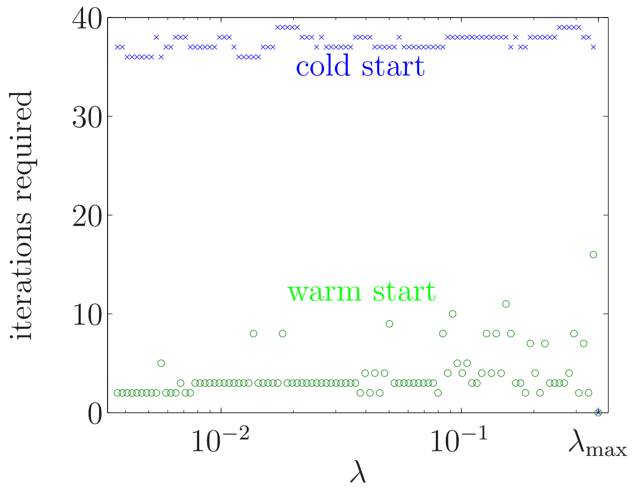

Figure 8: *Left.* Regularization path for leukemia cancer gene expression data. *Right.* Iterations required for cold-start and warm-start methods.

Our second example is the 20 Newsgroups data set, with $M = 100$ values of λ uniformly spaced on a logarithmic scale over $[0.05\lambda_{\max}, \lambda_{\max}]$. For this problem we have $\lambda_{\max} = 0.12$. The top plot in figure 9 shows the regularization path. The bottom left plot shows the total number of PCG iterations required to solve each problem, with the warm-start and cold-start methods. The bottom right plot shows the cardinality of w as a function of λ.

Here too the warm-start method gives a substantial advantage over the cold-start method, at least for λ not too small, *i.e.*, as long as the optimal weight vector is relatively sparse. The total runtime using the warm-start method is around 16 hours, and the total runtime using the cold-start method is around 33 hours, so the warm-start methods gives a savings of around $2 : 1$. If we consider only the range from $0.1\lambda_{\max}$ to $\lambda_{\max}$, the savings increases to $5 : 1$.

We note that for this example, the number of events (*i.e.*, a weight transitioning between zero and nonzero) along the regularization path is very large, so methods that attempt to track every event will be very slow.

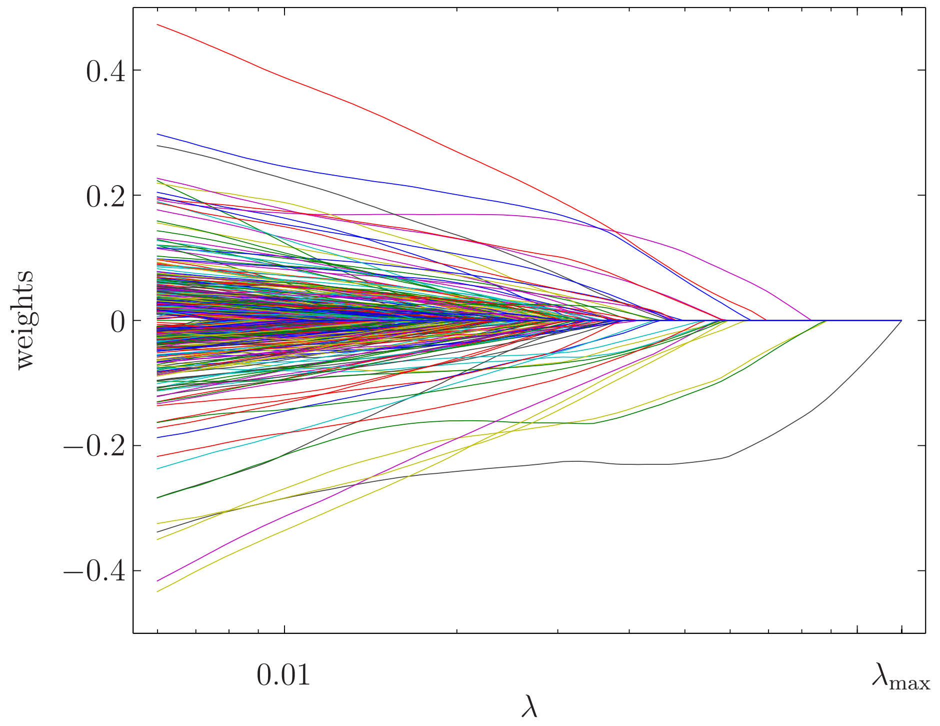

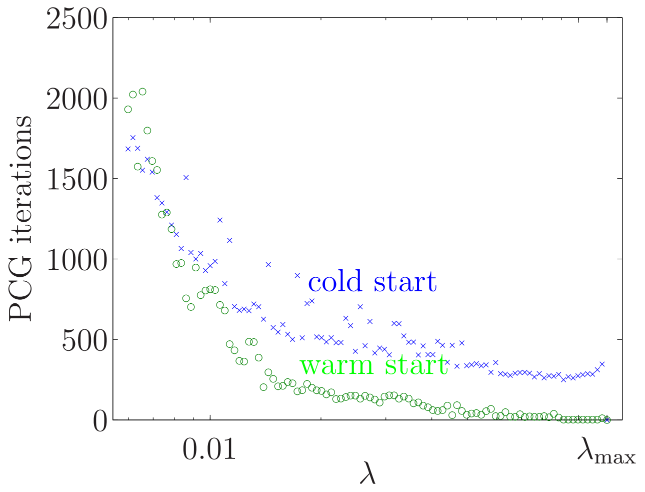

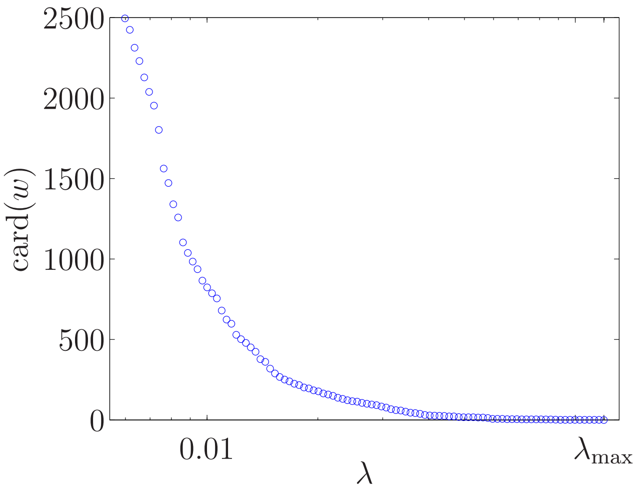

Figure 9: *Top.* Regularization path for 20 newsgroup data. *Bottom left.* Total PCG iterations required by cold-start and warm-start methods. *Bottom right.* card(w) versus λ.

7 Extensions and variations

The basic interior-point method and the truncated Newton variation can be extended to general ℓ_1-regularized convex loss minimization problems, with twice differentiable loss functions, that have the form

$$\begin{array}{ll} \text{minimize} & (1/m)\sum_{i=1}^m \phi(z_i) + \lambda\|w\|_1, \\ \text{subject to} & z_i = w^T a_i + v b_i + c_i, \quad i = 1,\ldots,m, \end{array} \tag{31}$$

with variables are $v \in \mathbf{R}$, $w \in \mathbf{R}^n$, and $z \in \mathbf{R}^m$, and problem data $c_i \in \mathbf{R}$, $a_i \in \mathbf{R}^n$, and $b_i \in \mathbf{R}$ determined by a set of given (observed or training) examples

$$(x_i, y_i) \in \mathbf{R}^n \times \mathbf{R}, \quad i = 1,\ldots,m.$$

Here $\phi : \mathbf{R} \to \mathbf{R}$ is a loss function which is convex and twice differentiable. Prior work related to the extension includes [43, 46].

In ℓ_1-regularized (binary) classification, we have $y_i \in \{-1,+1\}$ (binary labels), and z_i has the form $z_i = y_i(w^T x_i + v)$, so we have the form (31) with $a_i = y_i x_i$, $b_i = y_i$, and $c_i = 0$. The loss function ϕ is small and positive for positive arguments, and grows for negative arguments. When ϕ is the logistic loss function f, this general ℓ_1-regularized classification problem reduces to the ℓ_1-regularized LRP. The associated classifier is given by $y = \mathrm{sgn}(w^T x + v)$.

In linear regression, we have $y_i \in \mathbf{R}$, and z_i has the form $z_i = w^T x_i + v - y_i$, which is the difference between y_i and its predicted value, $w^T x_i + v$. Thus ℓ_1-regularized regression problems have the form (31) with $a_i = x_i$, $b_i = 1$, and $c_i = -y_i$. Typically ϕ is symmetric, with $\phi(0) = 0$. When the loss function is quadratic, *i.e.*, $\phi(u) = u^2$, the problem (31) is the l_1-regularized least squares regression problem studied extensively in the literature (see, *e.g.*, [20, 51]).

The dual of the problem (31) is

$$\begin{array}{ll} \text{maximize} & -(1/m)\sum_{i=1}^m \phi^*(-m\nu_i) + \nu^T c \\ \text{subject to} & \|A^T\nu\|_\infty \le \lambda, \quad b^T\nu = 0, \end{array} \tag{32}$$

where $A = [a_1 \ \cdots \ a_m]^T \in \mathbf{R}^{m\times n}$, the variable is $\nu \in \mathbf{R}^m$, and ϕ^* is the conjugate of the loss function ϕ,

$$\phi^*(y) = \sup_{u\in\mathbf{R}} \left(yu - \phi(u)\right).$$

As with l_1-regularized logistic regression, we can derive a bound on the suboptimality of (v, w), by constructing a dual feasible point $\bar\nu$, from an arbitrary w,

$$\bar\nu = (s/m)p(\bar v, w), \qquad p(\bar v, w) = \begin{bmatrix} \phi'(w^T a_1 + \bar v b_1 + c_1) \\ \vdots \\ \phi'(w^T a_m + \bar v b_m + c_m) \end{bmatrix},$$

where $\bar{v}$ is the optimal intercept for the offset w,

$$\bar{v} = \arg\min_v (1/m) \sum_{i=1}^{m} \phi(w^T a_i + v b_i + c_i),$$

and the scaling constant s is $s = \min\left\{m\lambda / \|A^T p(\bar{v}, w))\|_\infty, 1\right\}$.

Using this method for cheaply computing a dual feasible point and associated duality gap for *any* (v, w), we can extend the custom interior-point method for l_1-regularized LRPs to general ℓ_1-regularized convex (twice differentiable) loss problems.

Acknowledgments

This work is supported in part by the National Science Foundation under grants #0423905 and (through October 2005) #0140700, by the Air Force Office of Scientific Research under grant #F49620-01-1-0365, by MARCO Focus center for Circuit & System Solutions contract #2003-CT-888, and by MIT DARPA contract #N00014-05-1-0700. The authors thank Michael Grant, Trevor Hastie, Mee Young Park, and Yinyu Ye for helpful comments and suggestions.

References

[1] E. Allgower and K. Georg. Continuation and path following. *Acta Numerica*, 2:1–64, 1993.

[2] U. Alon, N. Barkai, D. Notterman, K. Gish, S. Ybarra, D. Mack, and A. Levine. Broad patterns of gene expression revealed by clustering of tumor and normal colon tissues probed by oligonucleotide arrays. *Proceedings of the National Academy of Sciences*, 96:6745–6750, 1999.

[3] P. Amestoy, T. Davis, and I. Duff. An approximate minimum degree ordering algorithm. *SIAM Journal on Matrix Analysis and Applications*, 17(4):886–905, 1996.

[4] S. Balakrishnan and D. Madigan. Algorithms for sparse linear classifiers in the massive data setting, 2005. Manuscript. Available from `www.stat.rutgers.edu/~madigan/papers/`.

[5] O. Banerjee, L. El Ghaoui, A. d'Aspremont, and G. Natsoulis. Convex optimization techniques for fitting sparse Gaussian graphical models. In *Proceedings of the 23rd International Conference on Machine Learning*, 2006.

[6] D. Bertsekas. *Nonlinear Programming.* Athena Scientific, second edition, 1999.

[7] J. Borwein and A. Lewis. *Convex Analysis and Nonlinear Optimization.* Springer, 2000.

[8] S. Boyd and L. Vandenberghe. *Convex Optimization.* Cambridge University Press, 2004. Available from `www.stanford.edu/~boyd/cvxbook`.

[9] S. Boyd, L. Vandenberghe, A. El Gamal, and S. Yun. Design of robust global power and ground networks. In *Proceedings of ACM/SIGDA International Symposium on Physical Design (ISPD)*, pages 60–65, 2001.

[10] K. Chaloner and K. Larntz. Optimal Bayesian design applied to logistic regression experiments. *Journal of Statistical Planning and Inferenc*, 21:191–208, 1989.

[11] S. Chen and D. Donoho. Basis pursuit. In *Proceedings of the Twenty-Eighth Asilomar Conference on Signals, Systems and Computers*, volume 1, pages 41–44, 1994.

[12] S. Chen, D. Donoho, and M. Saunders. Atomic decomposition by basis pursuit. *SIAM Review*, 43(1):129–159, 2001.

[13] A. Conn, N. Gould, and Ph. Toint. *LANCELOT: A Fortran package for large-scale nonlinear optimization (Release A)*, volume 17 of *Springer Series in Computational Mathematics*. Springer-Verlag, 1992.

[14] J. Dahl, V. Roychowdhury, and L. Vandenberghe. Maximum likelihood estimation of Gaussian graphical models: Numerical implementation and topology selection. Submitted. Available from `www.ee.ucla.edu/~vandenbe/covsel.html`, 2005.

[15] A. d'Aspremont, L. El Ghaoui, M. Jordan, and G. Lanckriet. A direct formulation for sparse PCA using semidefinite programming, 2005. In L. Saul, Y. Weiss and L. Bottou, editors, *Advances in Neural Information Processing Systems*, 17, pp. 41-48, MIT Press.

[16] R. Dembo and T. Steihaug. Truncated-Newton algorithms for large-scale unconstrained optimization. *Math. Program.*, 26:190–212, 1983.

[17] J. Demmel. *Applied Numerical Linear Algebra.* Society for Industrial and Applied Mathematics, 1997.

[18] D. Donoho and M. Elad. Optimally sparse representation in general (non-orthogonal) dictionaries via ℓ^1 minimization. *Proc. Nat. Aca. Sci.*, 100(5):2197–2202, March 2003.

[19] D. Donoho, I. Johnstone, G. Kerkyacharian, and D. Picard. Wavelet shrinkage: Asymptopia? *J. R. Statist. Soc. B.*, 57(2):301–337, 1995.

[20] B. Efron, T. Hastie, I. Johnstone, and R. Tibshirani. Least angle regression. *Annals of Statistics*, 32(2):407–499, 2004.

[21] H. Fu, M. Ng, M. Nikolova, and J. Barlow. Efficient minimization methods of mixed ℓ_1-ℓ_1 and ℓ_2-ℓ_1 norms for image restoration. *SIAM Journal on Scientific computing*, 27(6):18811902, 2006.

[22] A. Genkin, D. Lewis, and D. Madigan. Large-scale Bayesian logistic regression for text categorization, 2004. Manuscript. Available from `www.stat.rutgers.edu/~madigan/papers/`.

[23] A. George and J. Liu. *Computer solution of large sparse positive definite systems.* Prentice-Hall, 1981.

[24] P. Gill, W. Murray, M. Saunders, and M. Wright. User's guide for NPSOL (Version 4.0): A FORTRAN package for nonlinear programming. Technical Report SOL 86-2, Operations Research Dept., Stanford University, Stanford, California 94305, January 1986.

[25] T. Golub, D. Slonim, P. Tamayo, C. Gaasenbeek, J. Mesirov, H. Coller, M. Loh, J. Downing, M. Caligiuri, C. Bloomfield, and E. Lander. Molecular classification of cancer: Class discovery and class prediction by gene expression monitoring. *Science*, 286:531–537, 1999.

[26] A. Hassibi, J. How, and S. Boyd. Low-authority controller design via convex optimization. In *Proceedings of the IEEE Conference on Decision and Control*, pages 140–145, 1999.

[27] T. Hastie, S. Rosset, R. Tibshirani, and J. Zhu. The entire regularization path for the support vector machine. *Journal of Machine Learning Research*, 5:1391–1415, 2004.

[28] T. Jaakkola and M. Jordan. Bayesian parameter estimation via variational methods. *Statistics and Computing*, 10:25–37, 2000.

[29] S. Keerthi and D. DeCoste. A modified finite Newton method for fast solution of large scale linear SVMs. *Journal of Machine Learning Research*, 6:341–361, 2005.

[30] P. Komarek. *Logistic Regression for Data Mining and High-Dimensional Classification.* PhD thesis, Carnegie Mellon University, 2004.

[31] B. Krishnapuram, L. Carin, M. Figueiredo, and A. Hartemink. Sparse multinomial logistic regression: Fast algorithms and generalization bounds. *IEEE Transactions on Pattern Analysis and Machine Intelligence*, 27(6):957–968, 2005.

[32] B. Krishnapuram and A. Hartemink. Sparse multinomial logistic regression: Fast algorithms and generalization bounds. *IEEE Transactions on Pattern Analysis and Mach. Intelligence*, 27(6):957–968, 2005.

[33] K. Lang. Newsweeder: Learning to filter netnews. In *Proceedings of the twenty-first international conference on Machine learning (ICML)*, pages 331–339, 1995.

[34] M. Lobo, M. Fazel, and S. Boyd. Portfolio optimization with linear and fixed transaction costs. *Annals of Operations Research*, 2005.

[35] A. McCallum. Bow: A toolkit for statistical language modeling, text retrieval, classification and clustering. Available from `www.cs.cmu.edu/~mccallum/bow`, 1996.

[36] MOSEK ApS. *The MOSEK Optimization Tools Version 2.5. User's Manual and Reference*, 2002. Available from `www.mosek.com`.

[37] S. Nash. A survey of truncated-Newton methods. *Journal of Computational and Applied Mathematics*, 124:45–59, 2000.

[38] Y. Nesterov and A. Nemirovsky. *Interior-Point Polynomial Methods in Convex Programming*, volume 13 of *Studies in Applied Mathematics*. SIAM, Philadelphia, PA, 1994.

[39] D. Newman, S. Hettich, C. Blake, and C. Merz. UCI repository of machine learning databases, 1998. Available from `www.ics.uci.edu/~mlearn/MLRepository.html`.

[40] A. Ng. Feature selection, ℓ_1 vs. ℓ_2 regularization, and rotational invariance. In *Proceedings of the twenty-first international conference on Machine learning (ICML)*, pages 78–85, New York, NY, USA, 2004. ACM Press.

[41] J. Nocedal and S. Wright. *Numerical Optimization.* Springer Series in Operations Research. Springer, 1999.

[42] M. Osborne, B. Presnell, and B. Turlach. A new approach to variable selection in least squares problems. *IMA Journal of Numerical Analysis*, 20(3):389–403, 2000.

[43] M. Park and T. Hastie. An ℓ_1 regularization-path algorithm for generalized linear models, 2006. Manuscript. Available from `www-stat.stanford.edu/~hastie/Papers/glmpath.pdf`.

[44] B. Polyak. *Introduction to Optimization.* Optimization Software, 1987. Translated from Russian.

[45] L. Portugal, M. Resende, G. Veiga, and J. Júdice. A truncated primal-infeasible dual-feasible network interior point method, 1994.

[46] S. Rosset. Tracking curved regularized optimization solution paths. In L. Saul, Y. Weiss, and L. Bottou, editors, *Advances in Neural Information Processing Systems 17.* MIT Press, Cambridge, MA, 2005.

[47] S. Rosset, J. Zhu, and T. Hastie. Boosting as a regularized path to a maximum margin classifier. *Journal of Machine Learning Research*, 5:941–973, 2004.

[48] A. Ruszczynski. *Nonlinear Optimization.* Princeton university press, 2006.

[49] S. Shevade and S. Keerthi. A simple and efficient algorithm for gene selection using sparse logistic regression. *Bioinformatics*, 19(17):2246–2253, 2003.

[50] N. Z. Shor. *Minimization Methods for Non-differentiable Functions.* Springer Series in Computational Mathematics. Springer, 1985.

[51] R. Tibshirani. Regression shrinkage and selection via the Lasso. *Journal of the Royal Statistical Society, Series B*, 58(1):267–288, 1996.

[52] R. Tibshirani. The Lasso for variable selection in the Cox model. *Statistics in Medicine*, 16:385–395, 1997.

[53] R. Tibshirani, M. Saunders, S. Rosset, and J. Zhu. Sparsity and smoothness via the fused Lasso. *Journal of the Royal Statistical Society Series B*, 67(1):91–108, 2005.

[54] J. Tropp. Just relax: Convex programming methods for identifying sparse signals in noise. *IEEE Transactions on Information Theory*, 53(3):1030–1051, 2006.

[55] L. Vandenberghe and S. Boyd. A primal-dual potential reduction method for problems involving matrix inequalities. *Math. Program.*, 69:205–236, 1995.

[56] L. Vandenberghe, S. Boyd, and A. El Gamal. Optimizing dominant time constant in RC circuits. *IEEE Transactions on Computer-Aided Design*, 2(2):110–125, 1998.

[57] R. Vanderbei. *LOQO User's Manual — Version 3.10*, 1997. Available from `www.orfe.princeton.edu/loqo`.

[58] S. Wright. *Primal-dual interior-point methods.* Society for Industrial and Applied Mathematics, Philadelphia, PA, USA, 1997.

[59] Y. Ye. *Interior Point Algorithms. Theory and Analysis.* John Wiley & Sons, 1997.

[60] Z. Zhang, J. Kwok, and D. Yeung. Surrogate maximization/minimization algorithms for AdaBoost and the logistic regression model. In *Proceedings of the twenty-first international conference on Machine learning (ICML)*, pages 927–934, New York, NY, USA, 2004. ACM Press.

[61] J. Zhu, S. Rosset, T. Hastie, and R. Tibshirani. 1-norm support vector machines. In S. Thrun, L Saul, and B. Schölkopf, editors, *Advances in Neural Information Processing Systems 16*, pages 49–56, Cambridge, MA, 2004. MIT Press.